

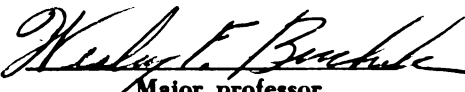
THE APPLICATION OF TILLAGE
ENERGY BY VIBRATION

Thesis for the Degree of Ph. D.
MICHIGAN STATE UNIVERSITY
James G. Hendrick, III
1962

This is to certify that the
thesis entitled
The Application of Tillage
Energy By Vibration

presented by
James G. Hendrick, III

has been accepted towards fulfillment
of the requirements for
Ph.D degree in Agricultural Engineering


Major professor

Date November 21, 1962

203

cut

THE APPLICATION OF TILLAGE
ENERGY BY VIBRATION

By

James G. Hendrick, III

AN ABSTRACT OF A THESIS

Submitted to
Michigan State University
in partial fulfillment of the requirements
for the degree of

DOCTOR OF PHILOSOPHY

Department of Agricultural Engineering

1962

Approved

Wesley F. Buckle *Mar 21, 1962*

ABSTRACT

THE APPLICATION OF TILLAGE ENERGY BY VIBRATION

by James G. Hendrick, III

Soil tillage requires more power than any other single agricultural operation. Any method which would reduce the power required to perform basic tillage operations could result in large savings to the American economy every year.

One method by which the efficiency of tillage can be increased is by transmitting energy from the tractor engine directly to the plow body by mechanical means. This would be more efficient than the present method of transmitting the energy through the soil-tire linkage, which has a relatively low efficiency.

In order to use the energy transmitted directly to the plow, the plow must be capable of imparting the energy to the soil. Tests were conducted to study the effect of applying energy by a vibrating plow body.

A model tillage tool, an inclined plane, was developed which could be vibrated in such a manner as to apply forces to the soil in a more efficient direction. Equipment and instrumentation were developed which permitted measurement of the individual forces acting upon the model tool. Laboratory tests were conducted using the model tool in a mobile soil bin to compare the draft force and energy requirement of a vibrating tillage tool with those of a rigid tillage tool.

James G. Hendrick, III

The draft force of the vibrating tool was found to be less than that of an identical rigid tool. The reduction in draft was a function of the soil parameters, vibrational frequency, and amplitude of vibration. The energy requirement of the vibrating tool was found to be less than that of a rigid tool at low frequencies, but became greater as the frequency was increased due to the formation of more soil shear planes and soil acceleration and deformation, especially at large amplitudes of vibration.

THE APPLICATION OF TILLAGE
ENERGY BY VIBRATION

By
James G. Hendrick, III

A THESIS

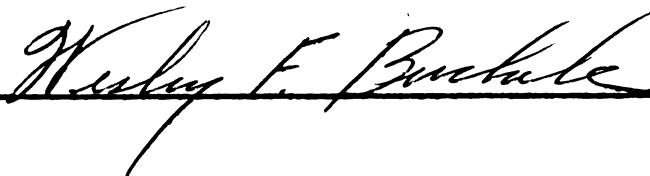
Submitted to
Michigan State University
in partial fulfillment of the requirements
for the degree of

DOCTOR OF PHILOSOPHY

Department of Agricultural Engineering

1962

Approved



ACKNOWLEDGMENTS

The author wishes to express his gratitude to the following people who assisted in this investigation and made the preparation of this thesis possible:

Dr. W. F. Buchele, the author's major professor, who provided guidance, encouragement, and enlightening discussions during this study.

Mr. C. M. Hansen, who served on the guidance committee and rendered many useful suggestions and gave encouragement on many occasions.

Major R. A. Liston of the U. S. Army Ordnance Tank-Automotive Command, who supported the project by lending instrumentation equipment.

Dr. L. E. Malvern and Dr. J. H. Stapleton, members of the guidance committee who contributed several helpful suggestions for the preparation of this manuscript.

Dr. A. W. Farrall, Head of the Agricultural Engineering Department, who gave support in providing the assistantship for this work.

Mr. A. C. Bailey and members of the staff who assisted in the construction of the necessary equipment.

Most especially to the author's wife, Kathy, who helped in the preparation of this manuscript, and whose loyalty, devotion, and understanding made this study possible.

L
R
E

T

R

S
C

TABLE OF CONTENTS

	Page
INTRODUCTION	1
REVIEW OF LITERATURE	4
EQUIPMENT AND PROCEDURES	11
Dynamometer	11
The Tillage Tool	20
Coefficient of Friction	27
Method of Vibration	29
Measurement of Vibrating Force	31
Soil Saw	37
Soil Bin	35
Soil Conditioning Equipment	39
Analog Computer	42
X-Y Plotter	45
THEORETICAL CONSIDERATIONS	49
Calculation of the Draft Force on a Rigid Tool	49
Discussion of Draft Reduction by a Vibrating Tillage Tool	51
RESULTS	55
Simulation of Cutting Resistance	55
Reduction of Draft Force	57
Energy Requirement of the Vibrating Blade	71
SUMMARY	79
CONCLUSIONS AND OBSERVATIONS	81
Conclusions	81

Obser

SUGGEST

REFEREN

APPEND

APPEND

TABLE OF CONTENTS (continued)

	Page
Observations	81
SUGGESTIONS FOR FURTHER INVESTIGATIONS	83
REFERENCES	84
APPENDIX A. Sample Problem	87
APPENDIX B. Tables	89

LIST OF TABLES

TABLE		PAGE
1.	Dynamometer and Pressure Cell Calibration	
	Information	89
2.	Tool Pressure Cell Calibration	90
3.	Normal Load vs. Tangential Force for Mild	
	Steel and Teflon at Various Moisture Contents .	91
4.	Force Exerted on the Blade by the Solenoid . . .	93
5.	Average Draft Values for a Rigid Tool Run at	
	30° and 40° Working Angles	94
6.	Energy Transmitted to the Blade by the	
	Solenoid in Soil at 17.5 % Moisture	94
7.	Relative Draft Data for a Working Angle (δ)	
	of 40° and 14 % Soil Moisture	95
8.	Relative Draft Data for a Working Angle (δ)	
	of 40° and 17.5 % Soil Moisture	97
9.	Relative Draft Data for a Working Angle (δ)	
	of 30° and 14 % Soil Moisture	99
10.	Relative Draft Data for a Working Angle (δ)	
	of 30° and 17.5 % Soil Moisture	101
11.	Tabulation of Values Used for Comparing	
	Measured Draft Force and Computed Draft	
	Force for a Rigid Blade (δ = 40°)	102
12.	Physical Description of Brookston Sandy	
	Loam Soil	103
13.	Bevometer Penetrometer Sinkage Data	104

FIGU

1.

2.

3.

4.

5.

6.

7.

8

9

10

11

L

LIST OF FIGURES

FIGURE		PAGE
1.	Reproduction of a Curve by Dubrovskii Showing the Relation Between Speed and Draft for Rigid and Oscillating Tillage Tools	6
2.	Force Diagrams of a Rigid and of a Vibrating Tillage Tool	9
3.	Strain Gage Dynamometer, Three-quarter View (62251-1)*	12
4.	Strain Gage Dynamometer, Bottom View (62251-3)	12
5.	Dynamometer Dimensions and Strain Gage Location	13
6.	Dynamometer Strain Gage Bridge Arrangement . . .	14
7.	Dynamometer Calibration Curve Where $\alpha = 72^\circ$, $x = 0.5'$ and $y = 1.0'$	17
8.	Dynamometer Calibration Curves for $\alpha = 90^\circ$, $x = 0.5'$, and $y = 1.0'$ and for $\alpha = 0^\circ$, $x = 0.5'$, and $y = 1.0'$	18
9.	Dynamometer Calibration Curve for $\alpha = 49^\circ$, $x = 0.5'$, and $y = 1.0'$	19
10.	The Instrumented Tillage Tool	21
11.	Tillage Tool in Mounted Position (6213661) . . .	22

* Numbers in parentheses refer to MSU Photo Lab negative numbers.

LIST OF FIGURES (continued)

FIGURE		PAGE
12.	Wiring Diagram of the Diaphragm Pressure Cell Strain Gage Bridge	24
13.	Method for Using a Mercury Column to Calibrate the Diaphragm Pressure Cells	25
14.	Calibration Curve for the Diaphragm Pressure Cells	26
15.	Method Used for Measuring Apparent Coefficient of Friction (μ^s)	28
16.	Apparent Coefficient of Friction of Brookston Sandy Loam on Polished Steel and on Teflon as a Function of Moisture Content	30
17.	The Soil Saw (62329-1)	34
18.	Soil Conditioning Equipment (62230-2)	34
19.	Schematic of the Mobile Soil Bin and Related Equipment	36
20.	Bevometer Used to Measure Soil Parameters (62128-7)	41
21.	General View of Recording Equipment (62532-1)	41
22.	Soil Parameters "c" and "Internal Angle of Friction" for Soil at 14 % Moisture and Bulk Densities of 1.12 and 1.23	43
23.	Soil Parameters "c" and "Internal Angle of Friction" for Soil at 17.5 % Moisture and Bulk Densities of 1.12 and 1.23	43

LIST OF FIGURES (continued)

FIGURES	PAGE
24. Wiring Schematic for Recording the Integrated Draft Signal	44
25. Mosley X-Y Plotter (A), Strain Gage Balance and Calibration Unit (B), and Performance Test Rig (C) (62264-3)	46
26. Strain Gage Balance and Calibration Unit Wiring Diagram	48
27. Performance Test Rig Wiring Diagram	48
28. Horizontal Force of Cutting for Two Wires As a Function of Velocity	56
29. Draft Ratios of a Vibrating and Rigid Tool for $\delta = 40^\circ$ and $\gamma = 10^\circ$	58
30. Draft Ratios of a Vibrating and Rigid Tool for $\delta = 40^\circ$ and $\gamma = 15^\circ$	59
31. Draft Ratios of a Vibrating and Rigid Tool for $\delta = 40^\circ$ and $\gamma = 20^\circ$	60
32. Relation of Draft Ratios for $\delta = 40^\circ$ and $\gamma = 10^\circ, 15^\circ$, and 20° at 14 % Soil Moisture . .	61
33. Relation of Draft Ratios for $\delta = 40^\circ$ and $\gamma = 10^\circ, 15^\circ$, and 20° at 17.5 % Soil Moisture	62
34. Draft Ratios of a Vibrating and Rigid Tool for $\delta = 30^\circ$ and $\gamma = 5^\circ$	63
35. Draft Ratios of a Vibrating and Rigid Tool for $\delta = 30^\circ$ and $\gamma = 10^\circ$	64

LIST OF FIGURES (continued)

FIGURE	PAGE
36. Draft Ratios of a Vibrating and Rigid Tool for $\delta = 30^\circ$ and $\gamma = 15^\circ$	65
37. Draft Ratios of a Vibrating and Rigid Tool for $\delta = 30^\circ$ and $\gamma = 20^\circ$	66
38. Relation of Draft Ratios for $\delta = 30^\circ$ and $\gamma = 5^\circ, 10^\circ, 15^\circ$, and 20° at 14 % Soil Moisture	67
39. Relation of Draft Ratios for $\delta = 30^\circ$ and $\gamma = 5^\circ, 10^\circ, 15^\circ$, and 20° at 17.5 % Soil Moisture	68
40. Percent Energy Applied by Draft and Solenoid Action of a Vibrating Tool Compared to a Rigid Tool Where $\delta = 40^\circ$ and $\gamma = 10^\circ$ at 17.5 % Soil Moisture	74
41. Percent Energy Applied by Draft and Solenoid Action of a Vibrating Tool Compared to a Rigid Tool Where $\delta = 40^\circ$ and $\gamma = 15^\circ$ at 17.5 % Soil Moisture	75
42. Percent Energy Applied by Draft and Solenoid Action of a Vibrating Tool Compared to a Rigid Tool Where $\delta = 40^\circ$ and $\gamma = 20^\circ$ at 17.5 % Soil Moisture	76

LIST OF FIGURES (continued)

FIGURE	PAGE
43. Percent Energy Applied by Draft and Solenoid Action of a Vibrating Tool Compared to a Rigid Tool Where $\delta = 30^\circ$ and $\theta = 10^\circ$ at 17.5 % Soil Moisture	77
44. Percent Energy Applied by Draft and Solenoid Action of a Vibrating Tool Compared to a Rigid Tool Where $\delta = 30^\circ$ and $\theta = 20^\circ$ at 17.5 % Soil Moisture	78

INTRODUCTION

Research workers in the field of tillage and soil mechanics have continually striven to reduce the draft and energy requirements of tillage tools. A recent concept under study is the vibration of tillage tools in which a portion of the tillage tool is moved in various planes by mechanical means.

One of the main disadvantages of basic tillage tools such as moldboard plows and subsoilers is the draft required to force them through the soil in a manner much like a rigid wedge. The drawbar pull of a tractor is limited by the soil-tire dynamics and the soil strength properties as well as by the power of the tractor engine. The draft of the tractor frequently can be increased by adding weight to the wheels; this, however, has the following objectionable results: (a) increased soil compaction, (b) increased mechanical impedance to plant roots, (c) reduced water infiltration rate, and (d) reduced air permeability and water holding capacity.

Most tractors develop maximum draft at 15 to 20 percent tire slip. The rolling resistance of the tractor consumes another 15 to 20 percent of the power. Thus the efficiency of a tractor in the field is the product of the above efficiencies (50 to 70 percent). Because mechanical power transmission is much more efficient, the tillage efficiency of the tractor-tool system could be increased by mechanically

by-passing the soil-tire relationship even if the efficiency of the tillage tool was not increased.

By imparting movement directly to the tillage tool the efficiency can be increased by: (a) applying forces in a more favorable manner, (b) separating the various forces acting on a tillage tool into their separate horizontal and vertical components by means of mechanical movement rather than by overcoming all of the forces by their horizontal component, i.e. draft, (c) breaking up the soil into smaller particles or clods.

Vibrating tillage tools offer these two basic advantages: (a) the farm tractor could reduce the drawbar pull of an implement by mechanical motion via the power-take-off shaft or other means, thus transmitting the engine power more effectively to the tool, and (b) the vibrating tillage tool breaks the soil into smaller particles or clods. This advantage offers the possibility of eliminating the need for secondary tillage operations.

A vibrating tillage implement could be pulled with light, high-powered tractors, which would result in reducing the soil compaction problem and reduce tractor cost.

The three basic objectives of this study were as follows: (1) to develop equipment and methods for measuring the forces acting on a simple tillage tool, (2) to develop a method for determining tillage forces and energy of rigid

and vibrating tools, and (3) to compare the energy requirements of rigid and vibrating tillage tools.

REVIEW OF LITERATURE

The first investigation concerning the application of mechanical movement to a tillage tool was conducted by Gunn and Tramontini (1955). They performed a series of experiments in which a simple, small blade (shaped like a subsoiler chisel) was attached to a vertical standard. The standard was pivoted at its upper end and connected to a pittman drive near the blade so that the blade and standard could be oscillated fore and aft at a controlled rate and frequency. The tests were run in relatively dense, dry soils; the amplitudes of the strokes most frequently used were 0.322 in. and 0.645 in.

The tests indicated that the average net draft could be greatly reduced by oscillating the experimental chisel. They reported that "the decrease was slight for oscillation velocities that were less than the tractor speed." A rapid reduction in draft occurred when the forward speed of the tractor was reduced in comparison with the oscillating velocity. The experimenters used several dimensionless parameters, one of which was:

$$K = \frac{V_t}{wr}$$

where: V_t = forward speed of the tractor, ft./sec.

w = the angular velocity of the pittman, radians per sec.

r = eccentricity of the crank, ft.

The greatest reduction in draft occurred when K had a value less than 1. That is, under conditions such that the maxi-

imum rearward velocity of the tool exceeded the forward speed of the tractor, which resulted in the tool's moving rearward with respect to the ground during a portion of its stroke.

Gunn and Tramontini found no large or significant reduction in total power due to the power required to oscillate the tool, but at a value of $K = 0.25$, a 60 percent reduction of draft was obtained. As the value of K increased, the amount of draft reduction decreased. Another result was that the oscillating tool appeared to give better soil fragmentation than a non-vibrating tool.

In an investigation by Dubrovskii (1956) a series of tests using a simple wedge-shaped model tool in sand were conducted using three modes of vibration: (a) the tool moved forward and back at an upward angle of about 45° to the horizontal, (b) the tool moved fore and aft, and (c) the tool moved in a "V" shaped path in which it was moved downward in the first portion of the stroke, and then upward. The greatest saving in draft occurred when using the first mode.

The results of Dubrovskii's experiment can be shown best by Figure 1, in which curve no. 1 is the non-oscillating relationship between draft and speed. Curves 2, 3, and 4 are draft curves at various frequencies of oscillation (mode of oscillation not specified). In all cases the vibrating tool resulted in a reduction of drawbar pull up to

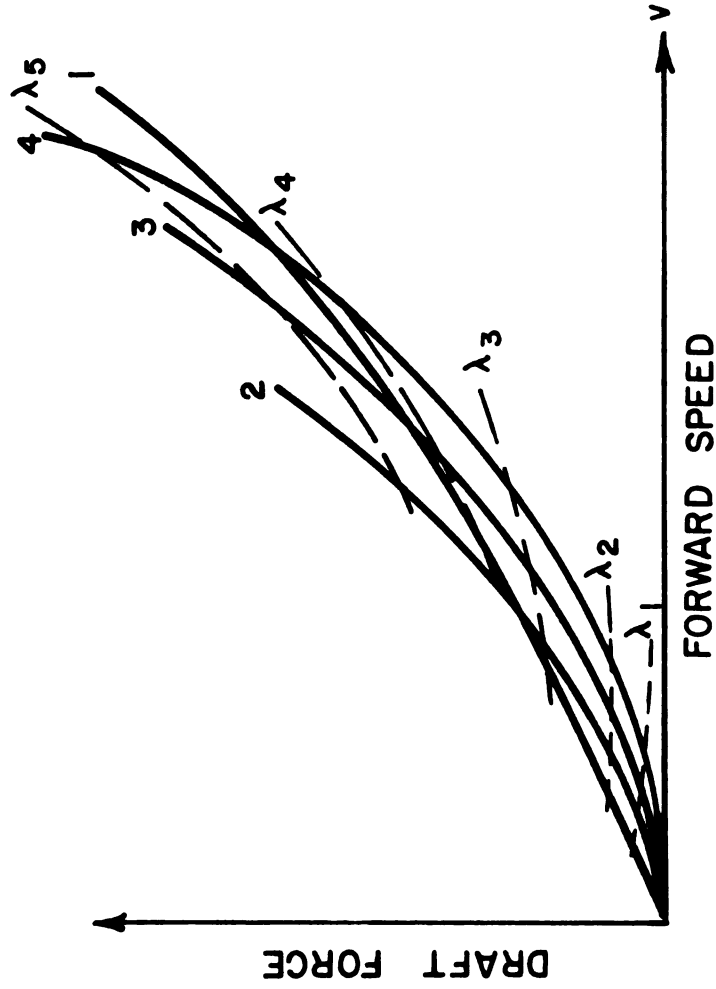


Figure 1. Reproduction of a curve by Dubrovskii showing the relation between speed and draft for rigid and oscillating tillage tools.

a certain forward speed and then showed an increase in drawbar pull beyond that speed.

The dashed curves in Figure 1 join points where the lengths of oscillation are equal. Dubrovskii noted that as these lines approached the non-vibratory curve, they merged with it, indicating that in actuality the operation of a rigid tool is a vibratory process. The experimental results showed that where the forced oscillation had a wave length with respect to forward travel less than the wave length of the shearing action of the rigid tool, the draft resistance was reduced.

Eggenmueller (1958) performed a series of tests with vibrating tillage tools in which the basic objectives were to reduce draft by the following tillage tool movements: (a) throwing soil upward so that at the instant the tool moved forward into untilled soil the tool surface was free of friction, (b) no lifting of the soil occurring during the forward tool motion, (c) reducing the cutting angle of the blade by driving it more directly into the soil, and (d) dividing the forces required for the individual processes of cutting, lifting, shearing, and accelerating the soil into distinct horizontal and vertical forces by means of the oscillating drive rather than by having the horizontal component overcome all forces as is the case with rigid tools. Figure 2 shows Eggenmueller's description of the

force components as presented by Soehne (1956) for the rigid tool and for the vibrating tool.

Eggenmueller considered various combinations of frequency, amplitude, direction of movement, and forward speed in a fine sandy loam under constant soil conditions. He found the direction of oscillation to be of particular importance, and that a direction of 30° to the horizontal was more favorable than a fore and aft movement in the reduction of draft. A movement as illustrated by Figure 2 B and C appeared to be the most favorable. Another important factor was the relationship between length of stroke and height of lift. A maximum ratio of 2 for length:height of stroke was recommended. A maximum reduction in draft of 75 percent was reported under optimal conditions.

Eggenmueller apparently did not consider the relationship between the natural frequency of shear plane formation and the frequency of forced vibrations; however, it was noted that the vibrational frequency required for the same reduction in draft increased with the forward speed of the vehicle. From charts in the text, the minimum reported frequency of 16 cycles per sec. appeared to be a little greater than the natural shear plane frequency of the soil at the maximum reported forward speed of 0.8 meters per sec.

He found that relatively small amplitudes of movement resulted in a considerable reduction in draft. From the power standpoint, it was preferable to operate at low fre-

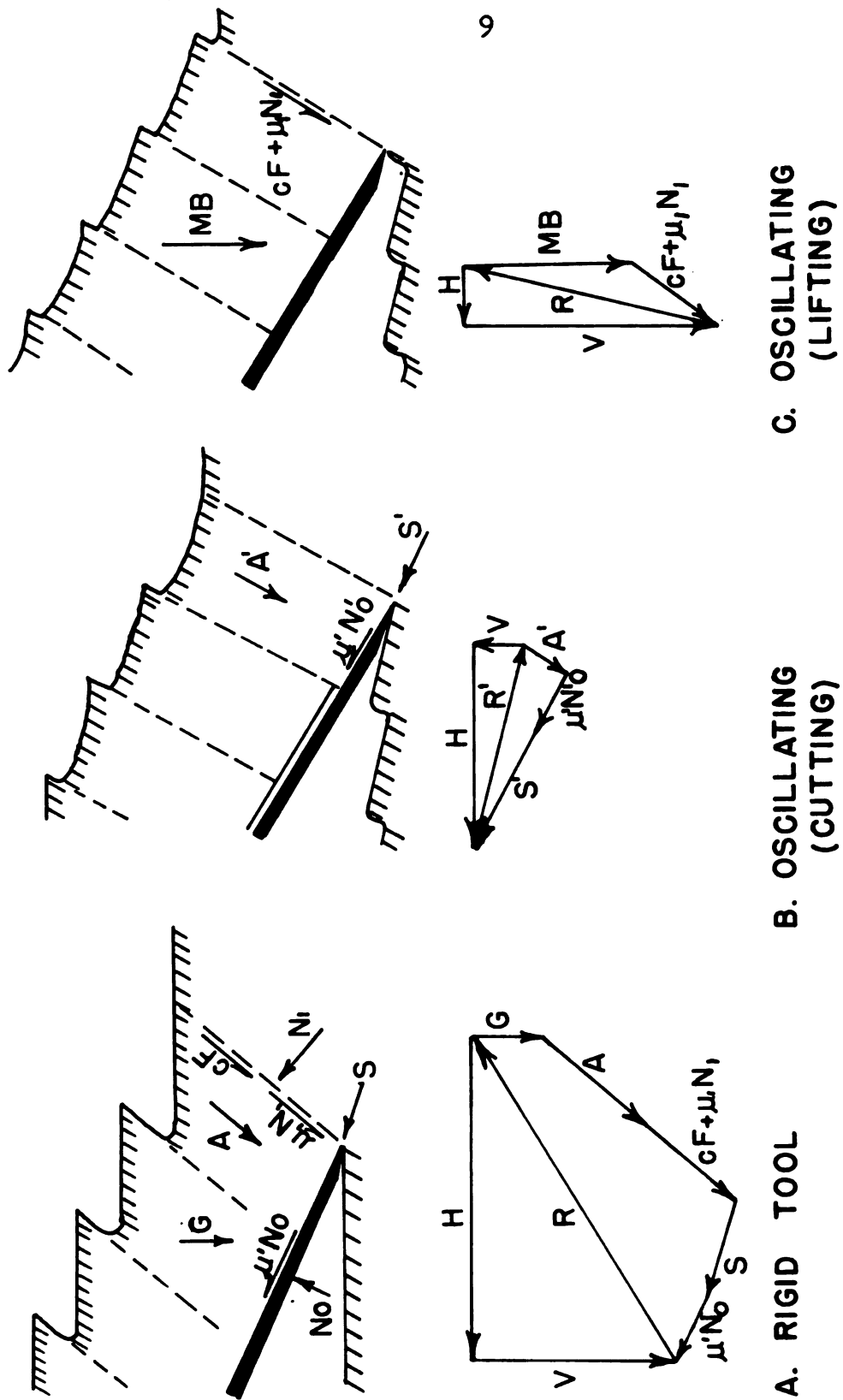


Figure 2. Force diagrams of a rigid and of a vibrating tillage tool.

quencies due to the movement of the soil mass, tool acceleration, etc. A reduction of 40 percent to 50 percent could be attained with the same total power input. Another factor mentioned was that soil crumbling and mixing appeared to be greater with the vibrating tool.

Hendrick (1960) found that a cohesive soil required less total energy to cause tensile failure at high loading rates. The ultimate stress was constant; the reduction in strain energy was obtained because the soil strained less under rapid loading rates.

EQUIPMENT AND PROCEDURES

Dynamometer.

In order to measure the soil forces acting on the tillage tool, a dynamometer (Figures 3 and 4) was constructed which could measure independently the vertical force, the horizontal force, and the moment about the dynamometer centerline caused by the resultant of the vertical and horizontal forces. The dynamometer was found to be independent of lateral forces and moments. By measuring these forces and moment, and by knowing the equation of the surface of the tillage tool (an inclined plane), the point of application of the resultant force on the tool surface could be calculated.

SR-4 strain gages were used as sensing elements to measure the strain in the dynamometer arms. Figure 5 is a drawing of the dynamometer showing strain gage placement. Figure 6 shows the arrangement of the three strain gage bridges used to yield the horizontal force, vertical force, and the bending moment independently. Gages 1, 2, 3, and 4 sensed the strain in the dynamometer arms due to forces in the horizontal plane in the direction of travel (draft). Gages 5, 6, 7, and 8 sensed the strain in the dynamometer arms due to vertical forces. Gages 9, 10, 11, and 12 sensed the strain in the dynamometer arms due to the moment caused by applied forces about a lateral axis through the dynamometer centerline.

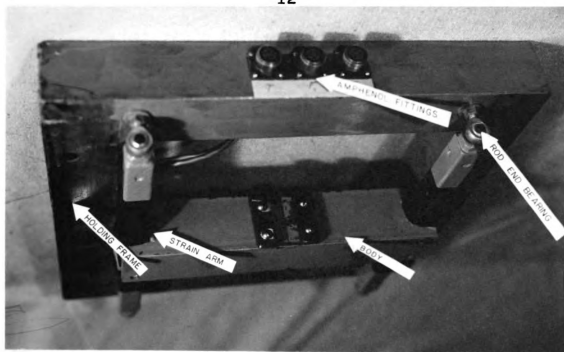


Figure 3. Strain gage dynamometer, three-quarter view.

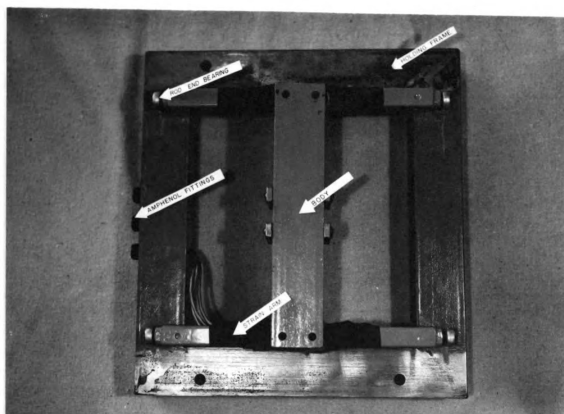


Figure 4. Strain gage dynamometer, bottom view.

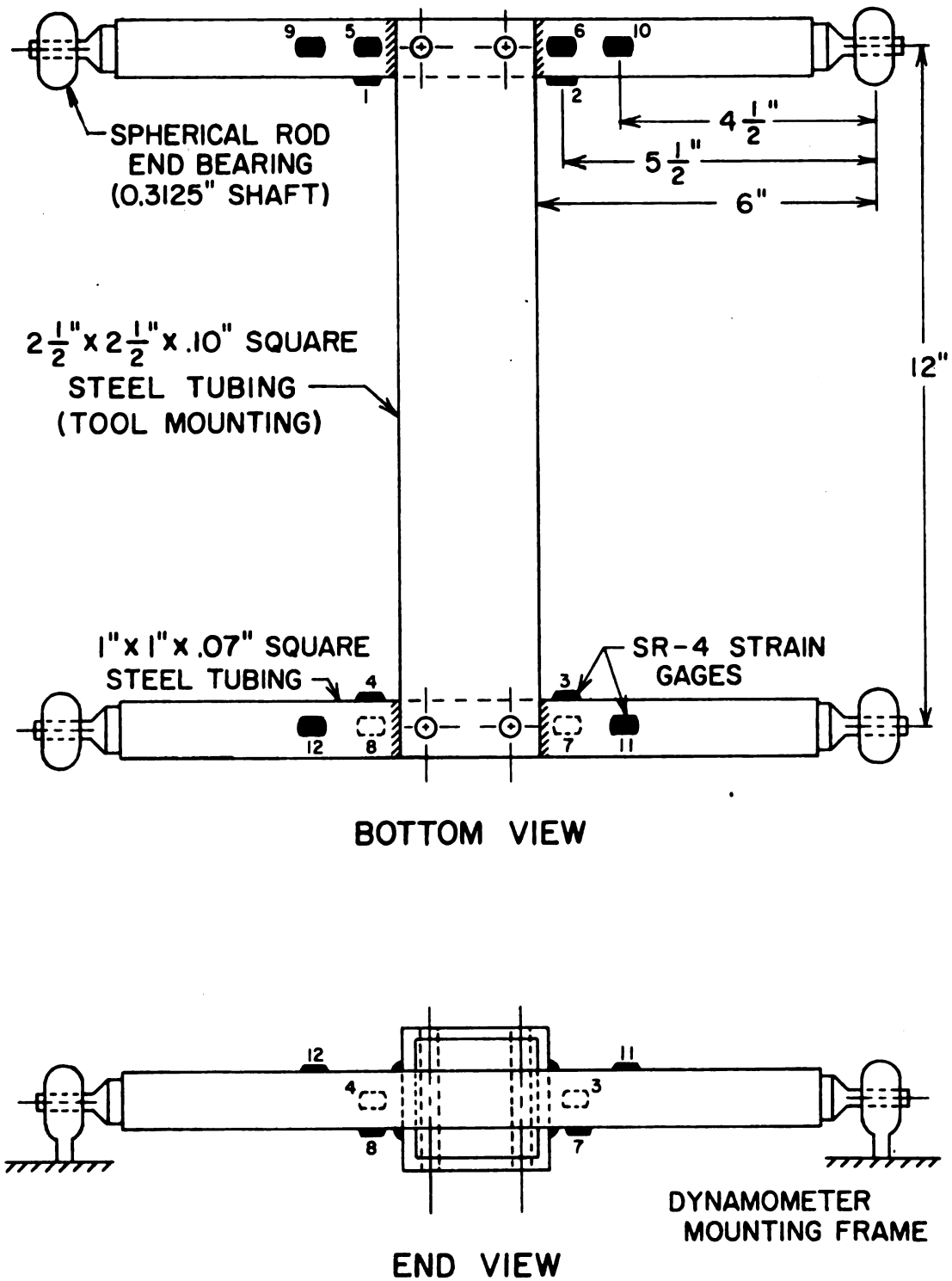


Figure 5. Dynamometer dimensions and strain gage location.

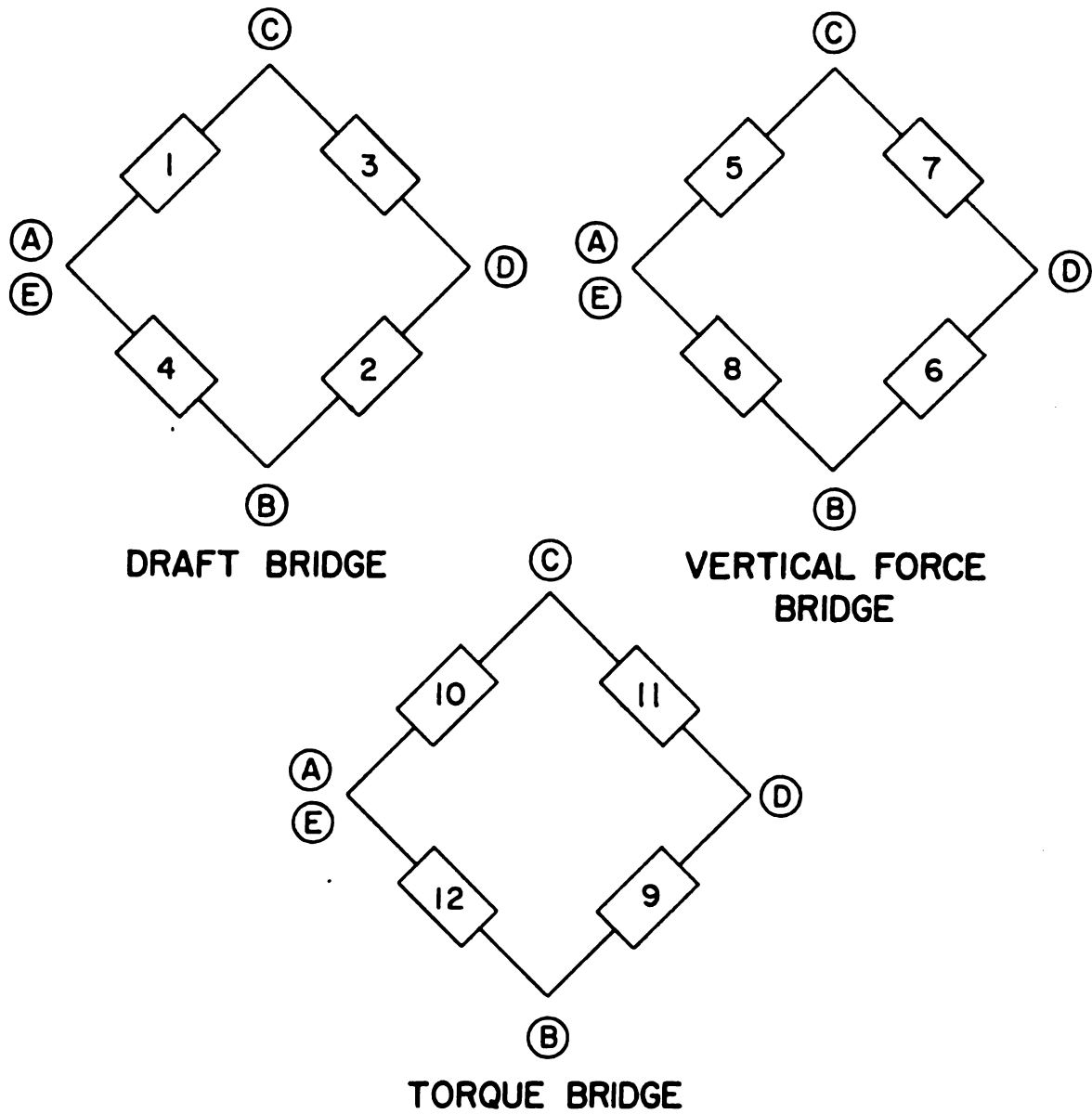


Figure 6. Dynamometer strain gage bridge arrangement.

The body of the dynamometer was made of 2-1/2 in. x 2-1/2 in. x 0.10 in. square steel tubing (weight per ft. = 3.2 lbs.). The strain arms (Figure 5) of the dynamometer were made of 1 in. x 1 in. x 0.070 in. square steel tubing. The square steel tubing increased the rigidity and sensitivity of the dynamometer while the weight was reduced; this increased the resonant frequency of the body. The resonant frequency of the dynamometer with a tillage tool attached was determined by applying a force and removing it suddenly. The resulting oscillograph trace showed a resonant frequency of 55 cps. To check the frequency response of the oscillograph, a cathode ray oscilloscope was attached to the draft-measuring channel of the oscillograph and polaroid pictures were made of the oscilloscope trace as the tool was vibrated. The recordings of the oscilloscope and of the oscillograph were compared and found to be identical provided the maximum pen deflection of the oscillograph was limited to 15 mm.

The outer ends of the strain arms were fitted into spherical rod end bearings. The strain arms thus acted as cantilever beams fixed at the dynamometer body and free at the end in the bearings.

The tillage tool standard was clamped to the dynamometer body in such a manner that the axis of rotation of the tool was directly below the lateral axis of symmetry of the dynamometer.

A series of calibration tests were made and the results are shown in Figures 7, 8, and 9. The dynamometer was calibrated by applying a known force (F) at a known angle (α) to the horizontal (Figure 7), and at a known location with respect to the dynamometer centerlines (x and y). The horizontal and vertical measurements were found to be independent of one another, and the results of measured torque and calculated torque were found to be in agreement within 2 percent. Table 1 contains calibration data for each of the recorded forces.

The line of the resultant force could be determined from the recorded forces when the equation of the plane of the tillage tool was known. The point of application of the resultant force on the tillage tool could be calculated. Appendix A shows a sample calculation.

To determine the rigidity of the dynamometer, a force of 160 pounds was applied in a horizontal direction (F_x) at $y = 1.0$ ft.; the deflection along the line of travel was 0.06 in. With $F_y = 160$ lbs. and $y = 0.0$ ft., the vertical deflection was 0.06 in.

The maximum sensitivity of the dynamometer was calculated to be 2.5 mm deflection on the oscillograph per pound applied in either the longitudinal or the vertical direction. The maximum sensitivity as determined by calibration was 3.5 mm deflection per pound.

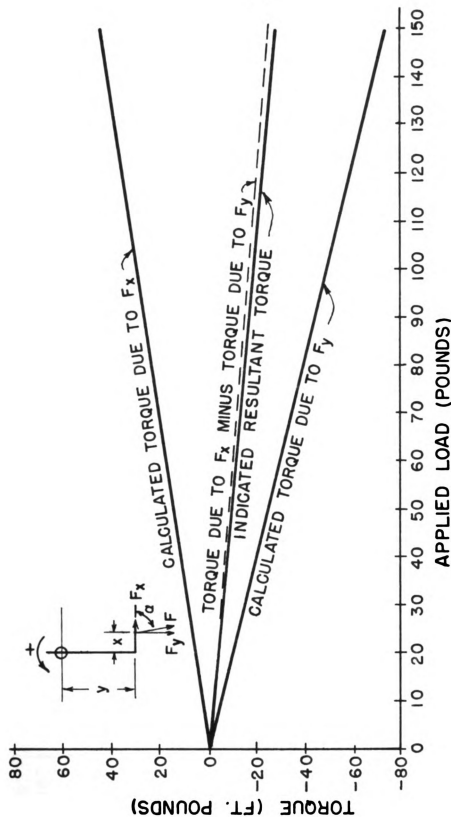


Figure 7. Dynamometer calibration curve where $a = 72$, $x = 0.5'$, and $y = 1.0'$.

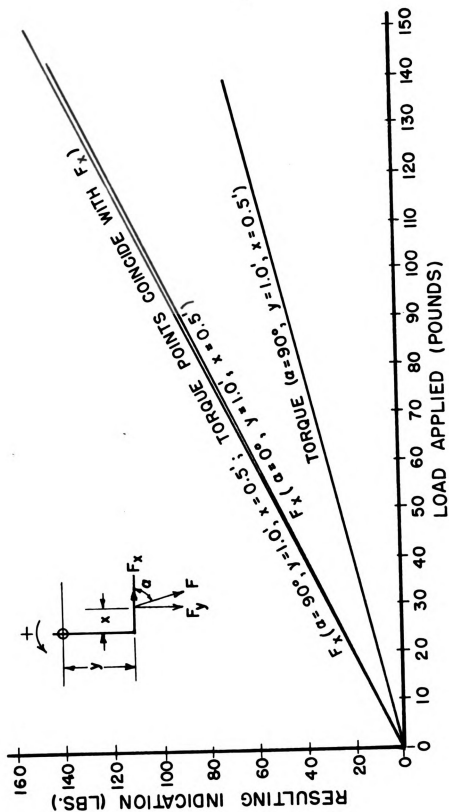


Figure 8. Dynamometer calibration curves for $a = 90^\circ$, $x = 0.5'$, and $y = 1.0'$ and for $a = 0^\circ$, $x = 0.5'$, and $y = 1.0'$.

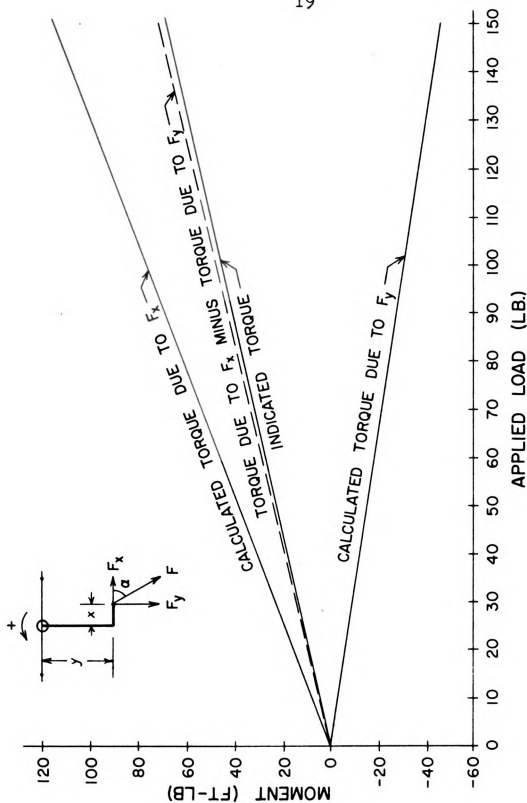


Figure 9. Dynamometer calibration curve for $\alpha = 49^\circ$, $x = 0.5'$, and $y = 1.0'$.

The Tillage Tool.

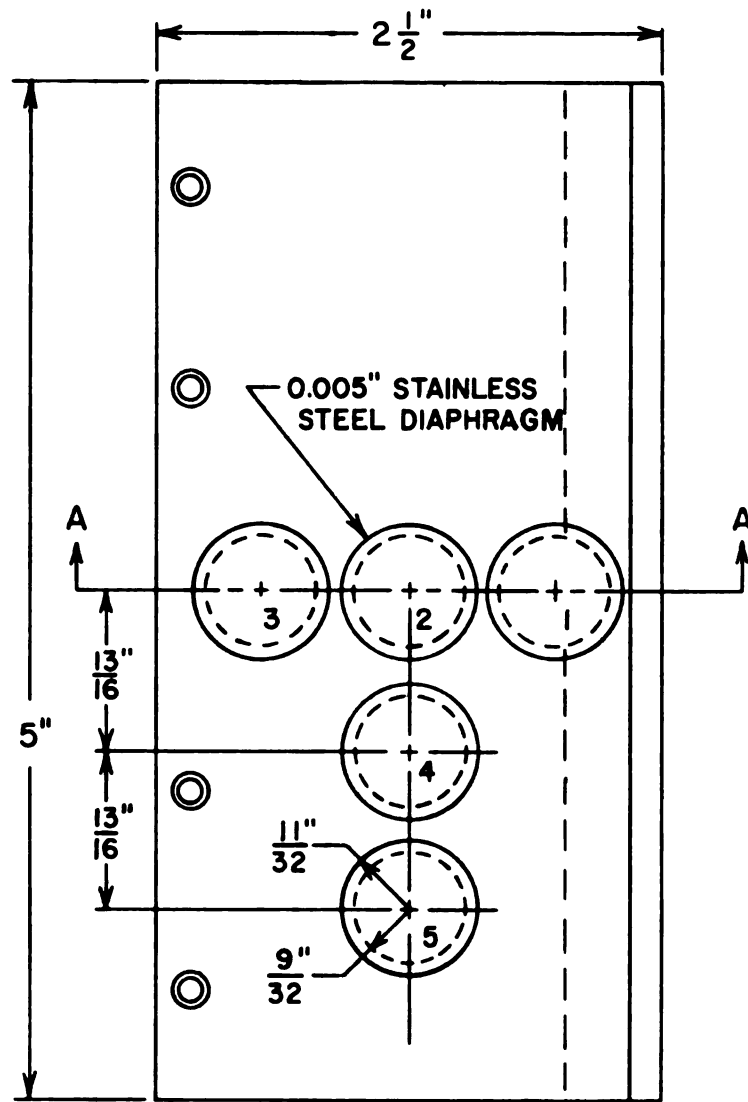
The simple tillage tool designed for this investigation is illustrated in Figure 10. The dimensions of the mild steel tool were $3/16$ in. thick, 5 in. wide, and $2-1/2$ in. long. The forward edge was machined to a $1/64$ in. radius and blended into a 20° bevel. The tool was mounted in bearings located at the rear edge. It rotated in the bearings about an axis through the top surface of the tool (Figure 11). When the tool was rotated, the forward edge of the tool swung upward describing an arc.

This method of tool movement was employed for three reasons: (1) the maximum displacement of the soil was in the region of the shear plane, (2) maximum acceleration of the soil mass occurred only at the cutting edge of the tool, and (3) rigid mounting of the standard minimized the tool mass to be actuated.

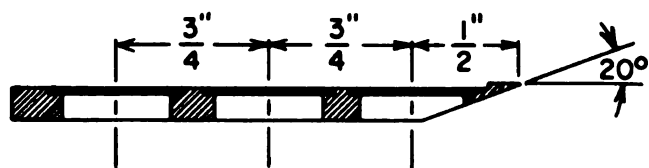
In order to measure the forces acting normal to the tool surface, a series of five diaphragm pressure cells were provided as illustrated (see Figure 10). The diaphragms were made of 0.005 in. thick stainless steel shim stock. In order to make the diaphragms flush with the tool surface, the $9/16$ in. holes were counterbored to $5/8$ in. diameter and 0.006 in. deep and the round shim stock diaphragms were silver-soldered into place.

The tool was covered with a 4 mil layer of pressure sensitive Teflon. The Teflon layer reduced the sliding re-

21



TOP VIEW



SECTION A-A

Figure 10. The instrumented tillage tool.

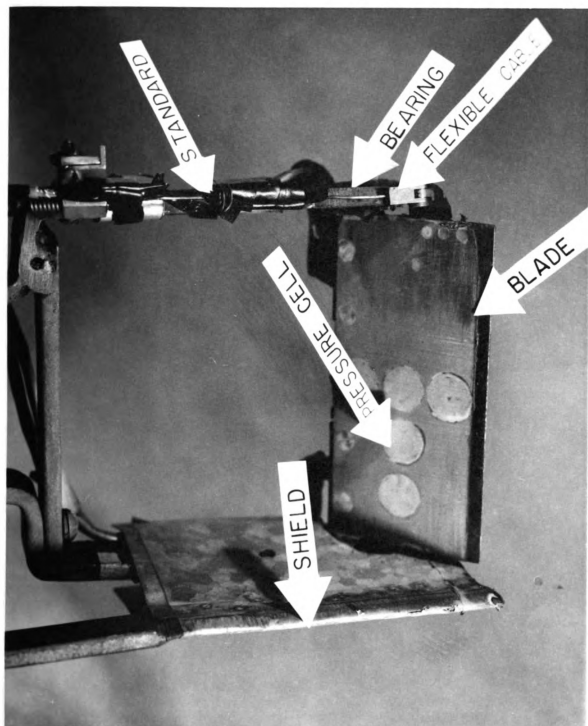


Figure 11. Tillage tool in mounted position.

sistance of the soil on the tool face and smoothed the slight imperfections which developed during soldering the pressure diaphragms onto the tool. It also prevented soil from sticking to the surface and "bridging over" the pressure cells. In order to prevent the leading edge of the Teflon layer from being disturbed or peeled off by the soil, a 0.006 in. layer of steel was machined from the tool face a distance of 1/4 in. behind the leading edge (Figure 10). This permitted the leading edge of the Teflon layer to be protected by steel and thus remain in place.

Sanders-Roe foil diaphragm strain gages (Radshaw 1/2-2ED) were attached to the underside of each diaphragm to measure the diaphragm strain. Figure 12 shows the wiring diagram for the pressure cell bridges. Calibration of the pressure cells showed them to be linear within 4 percent up to 15 psi (this was well above the unit pressures recorded during the tests). A method of calibrating the pressure cells was devised in which a column of mercury was used to provide a known unit pressure. Figure 13 shows a schematic of the system employed. By setting the height of the mercury column, the normal pressure on each cell was determined. The calibration curve for the five pressure cells is shown in Figure 14; each point is the average of four tests. Table 2 contains the individual readings for each cell. The maximum sensitivity was found to be 10 mm deflection per psi.

24

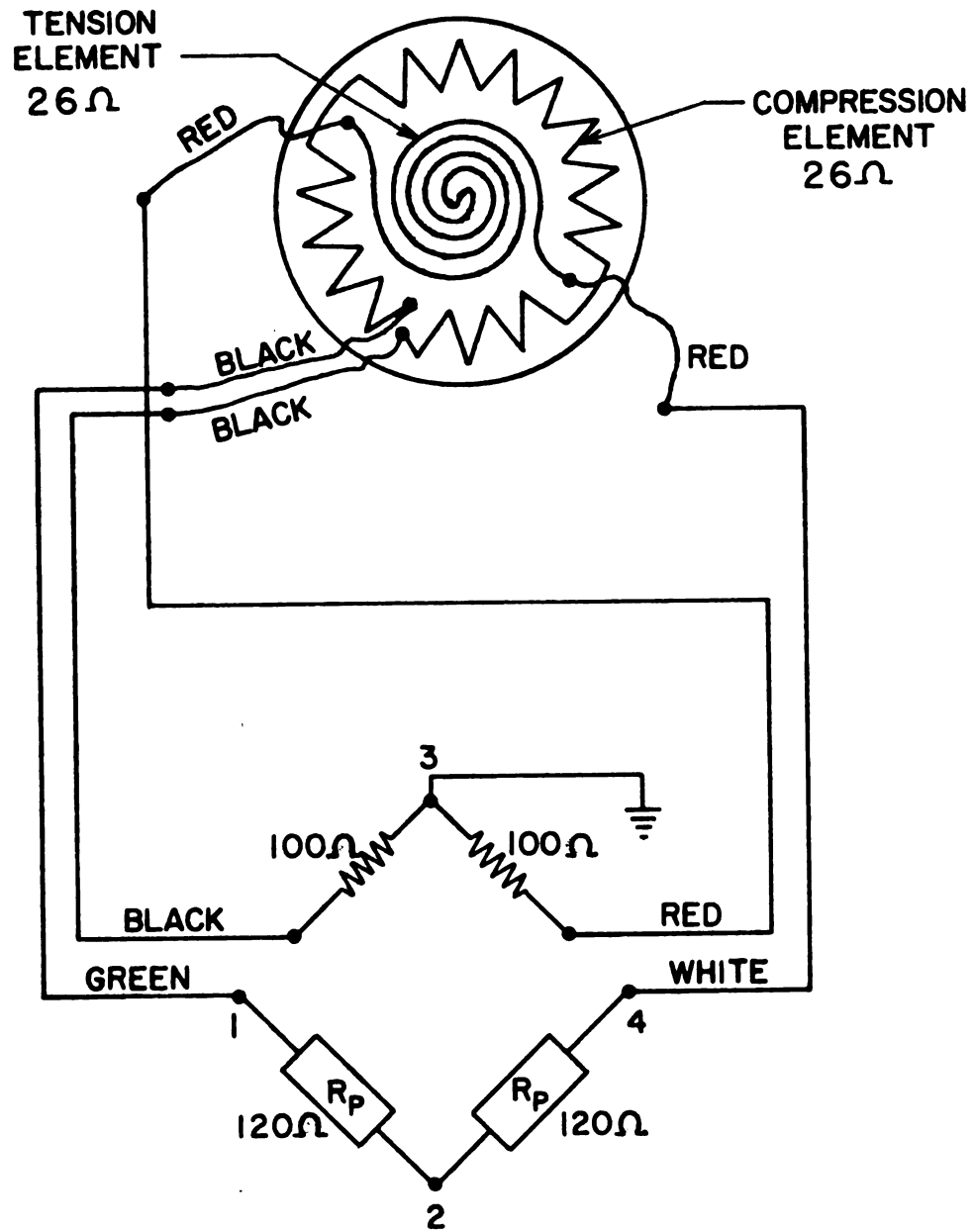


Figure 12. Wiring diagram of the diaphragm pressure cell strain gage bridge.

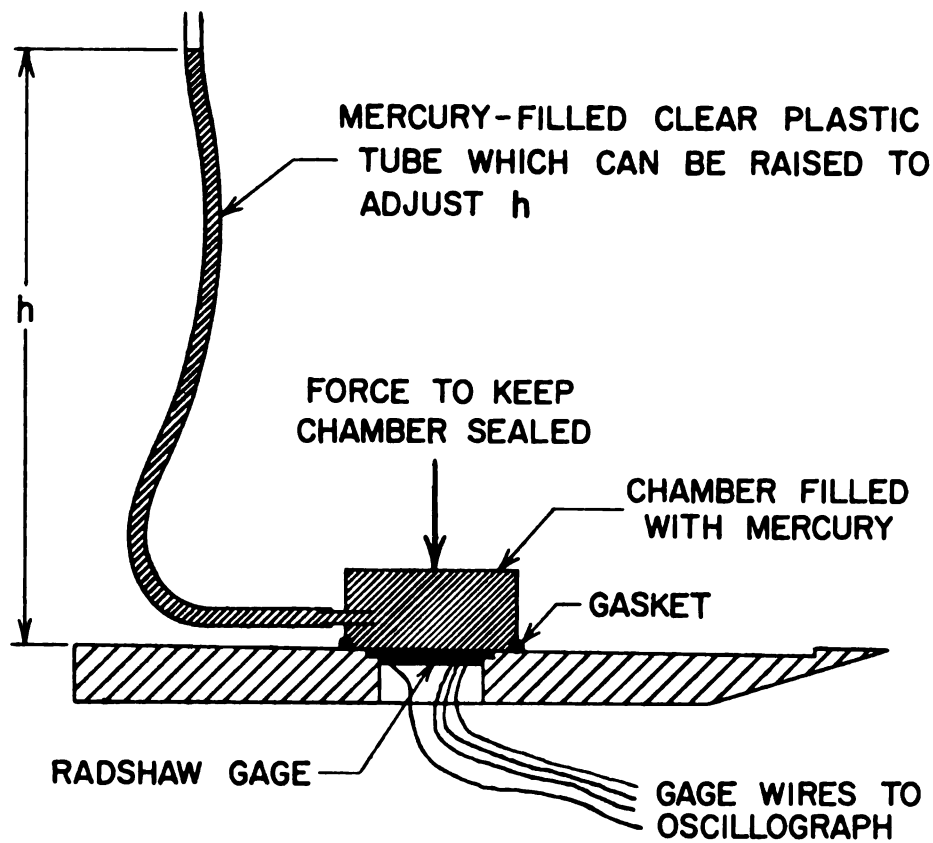


Figure 13. Method for using a mercury column to calibrate the diaphragm pressure cells.

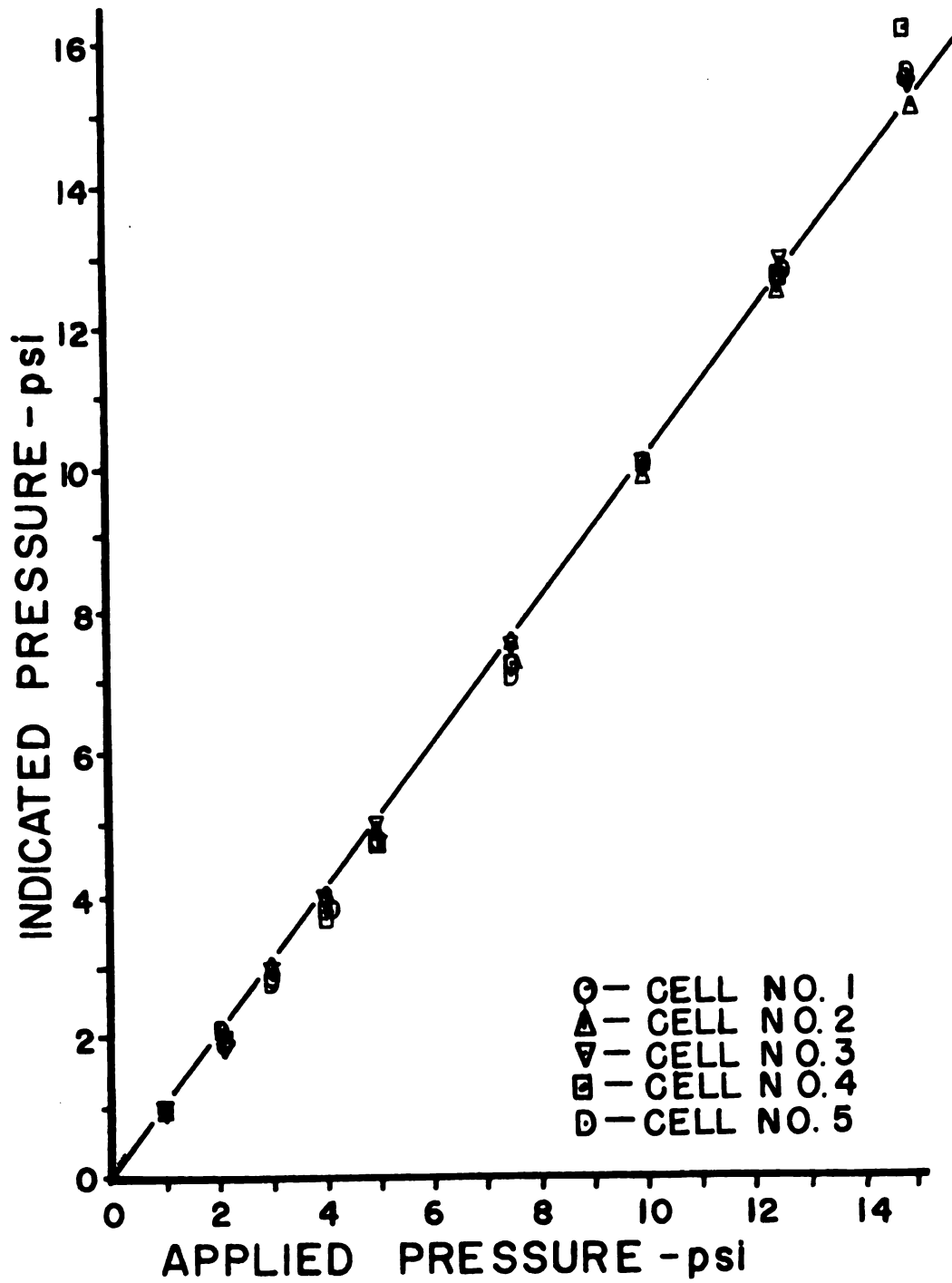


Figure 14. Calibration curve for the diaphragm pressure cells.

Another method was used to check the calibration of the pressure cells at frequent intervals. A 3/8 in. thick layer of foam rubber was cut to fit over a cell. A Soil-test model CL-700 penetrometer was pressed on the center of each rubber-covered cell until a penetrometer reading of 4.5 was registered. This force then corresponded to a normal load on the tool of 10 psi. The pressure cells were found to be in calibration each time they were tested.

A second tool was made of thinner material, sharpened to a more acute angle and not fitted with pressure cells. This tool was used for working at more acute angles to the horizontal than the instrumented tool.

Coefficient of Friction.

The apparent coefficient of friction (μ') of the soil on the Teflon layer of the tillage tool had to be determined in order to calculate the energy expended in overcoming the sliding resistance of the soil on the tool face. A series of tests was run to find the apparent coefficient of friction, and to compare the friction of Teflon with that of steel. Figure 15 shows a schematic of the method used. The soil sample was loaded with the normal force (N), and then pulled first along the steel surface and then across the Teflon surface. The bottom of the sample was shaved off after each test to provide a fresh soil surface for the next test.

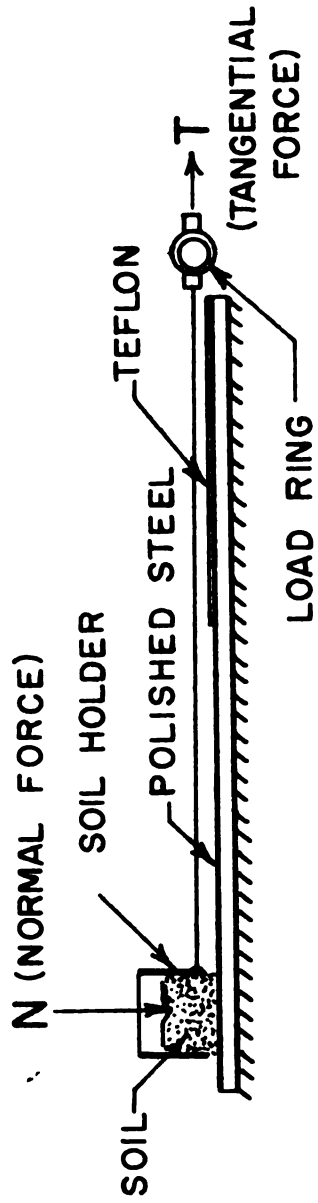


Figure 15. Method used for measuring apparent coefficient of friction (μ').

Three replications each were run at three normal weights ($N = 2.2 \text{ lb.}, 5.2 \text{ lb.}, 7.2 \text{ lb.}$) and at seven moisture contents (0.65 %, 6.0 %, 9.1 %, 11.4 %, 15 %, 19.7 %, and 26.5 %) on a dry weight basis. The graphs illustrating the results for both polished mild steel and Teflon are shown in Figure 16, and the data are presented in Table 3. These results agree closely with those of Nichols (1931) for a soil having 16 percent colloid; the soil used in this experiment contained 17 percent colloid, Stong (1960). Nichols proposed four basic phases of soil and metal friction. These phases were the compression phase, the friction phase, the adhesion phase, and the lubrication phase. This investigation was concerned with the last three phases.

According to Nichols, the friction phase is from 0 % to 7.5 % moisture, the adhesion commences at 7.5 % and increases to a maximum at 14 % moisture for a soil with 17 % colloid content. The results of this investigation had a close correlation with those of Nichols. Nichols found the average apparent coefficient of friction in the friction phase to be 0.40 for soil on steel. For the adhesion phase the maximum coefficient of friction was 0.56. Excess moisture causes a film of water to reduce the coefficient of friction in the lubrication phase.

Method of Vibration.

The plunger of an electrical solenoid was attached to one edge of the tillage tool by a flexible cable (Figure 11).

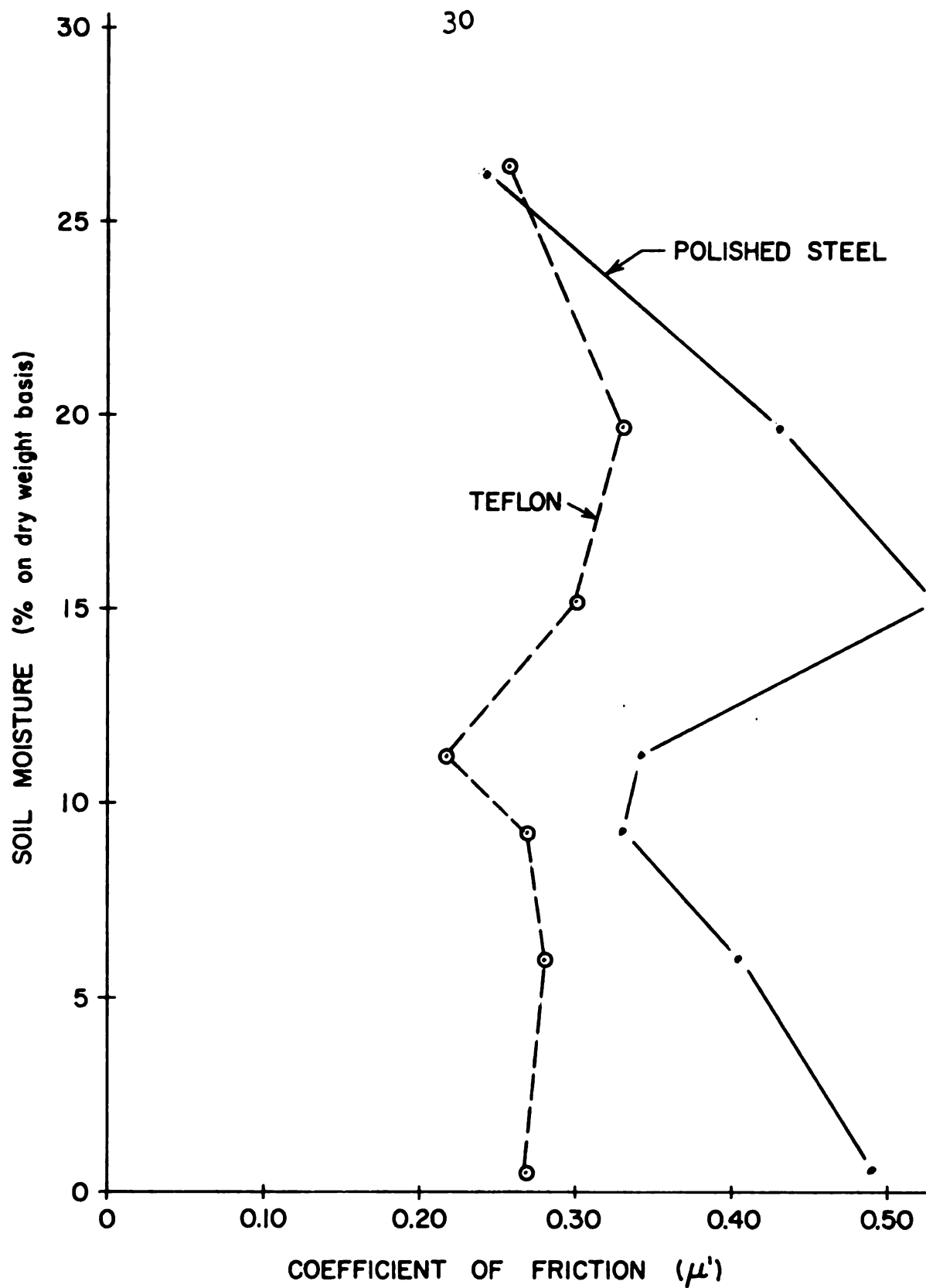


Figure 16. Apparent coefficient of friction of Brookston Sandy Loam on polished steel and on Teflon as a function of moisture content.

By attaching the cable casing to the tool standard and the wire to the tillage tool, the dynamometer measured the forces acting upon the blade without a noticeable disturbance from the transmitting force. When the solenoid was actuated, the plunger was drawn into the coil and the movement was transmitted to the blade via the cable, causing the blade to pivot about its axis and to swing the tip up and forward. To control the solenoid frequency, a universal electric motor was connected to a variable voltage source. The motor rotated a cam which activated a switch in the solenoid circuit and permitted frequencies of 2 cps to 21 cps. Another switch in the solenoid circuit permitted the vibrations to be stopped at short intervals so that both vibratory and non-vibratory tests could be run for short distances in one pass of the soil bin. During a test, the tool was operated as a series of rigid and vibrating tools. The forces acting on the vibrating tool were then compared with those of a rigid tool.

Displacement of the tool tip was controlled by regulating the movement of the solenoid plunger. Angular rotations of the blade of 5° , 10° , 15° , and 20° were used.

Measurement of Vibrating Force.

In order to measure the actual pull exerted on the tool by the solenoid during each stroke, a metal strip was instrumented with strain gages and mounted on the lower end of the flexible cable adjacent to the tillage tool. The

solenoid could thus be actuated with the tool removed from the soil and the force required to accelerate the tool was determined by observing the strain gage signal on an oscilloscope. The tool was next placed in loose soil and the solenoid actuated again. The resultant force represented the force required to accelerate the blade and the soil. The blade was then moved into the soil under test conditions and the solenoid activated again. The resultant force represented the force required to accelerate the blade and soil and to cause a shear plane failure. In this manner the various components of energy of the solenoid stroke could be computed when the length of stroke was known. Table 4 contains the data from tests of all three blade conditions and for various angles of movement of the blade tip. In all cases the shape of the force curve observed on the oscilloscope was that of a sine wave; therefore, by observing the maximum force, and multiplying by .636 the average force of the solenoid could be obtained. The duration of the applied force was 2.0 ± 0.1 milli-seconds in all cases.

Soil Saw.

In order to investigate the forces acting only on the model tillage tool, a method had to be devised whereby the tool standard or supports would not pass through the soil and cause extra forces to be recorded.

A device was designed and constructed which cut two 1-in. wide trenches in the soil and left a 4-in. wide undisturbed section of soil between them. The tool standards were positioned in the trenches and the tillage tool, held between the standards, cut the center section of soil.

This method also resulted in the soil shear planes developed by the tool being relatively straight, and not crescent-shaped as would be the case if the tool were operated in a solid soil mass. Since the soil shear planes were nearly flat and straight, the calculation of the unit force required to form each shear plane was simplified.

The Soil Saw (Figure 17) was constructed of two flat plates with teeth of angle iron welded radially to the plates. Spacers were placed between the plates to control the width of undisturbed soil section. The saw was mounted on a shaft placed across and above the soil bin and rotated by an electric motor. The direction of rotation was such that the bottom teeth of the Soil Saw moved in a direction opposite to the movement of the bin; the soil was cut loose, picked up, and thrown upward and forward. A metal hood was placed over the Soil Saw to prevent soil from being thrown out of the bin.

At first, loose soil struck the metal hood and fell back onto the soil slice to be investigated. A metal strip was placed between the blades of the Soil Saw so that it swept away the fall-back with each rotation and thus re-

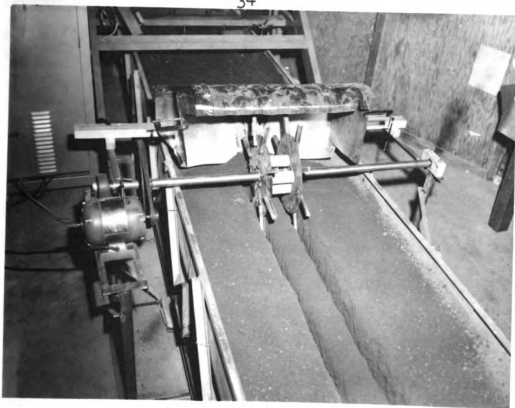


Figure 17. The soil saw.

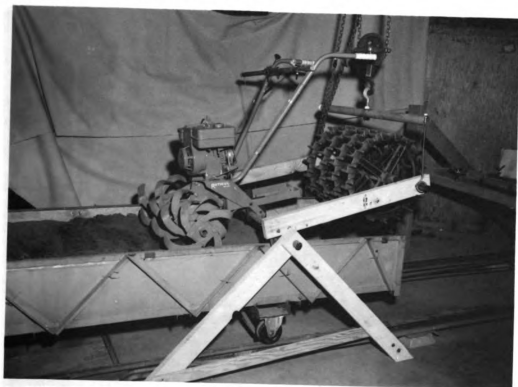


Figure 18. Soil conditioning equipment.

moved the excess soil from the top of the test area, and planed the top surface of the test section to provide a means of controlling the section height to within $\pm 1/16$ in.

Some loose soil fell back into the trenches even with these precautions; therefore, the tool standards were protected by rigid metal shields which were connected to the dynamometer holding frame. The shield prevented the loose soil from contacting the standards and causing erroneous indications of forces acting on the blade.

Careful inspection did not show any cracks, ruptures, or irregularities in the soil section resulting from the operation of the soil saw.

Another advantage of the Soil Saw was that each pass of the tool disturbed only a narrow section of soil, i.e. the width of the undisturbed center section plus the two trenches. After each pass of the tool the Soil Saw was moved laterally until one set of teeth was positioned to cut in a previously opened trench; the other set of teeth cut a new trench. Four series of tests were run side by side before the soil had to be processed. Still another advantage of this method was that no effects were caused by the proximity of the tool to the bin sides.

Soil Bin.

In order to simplify instrumentation and to facilitate soil handling, a mobile soil bin was constructed. Figure 19

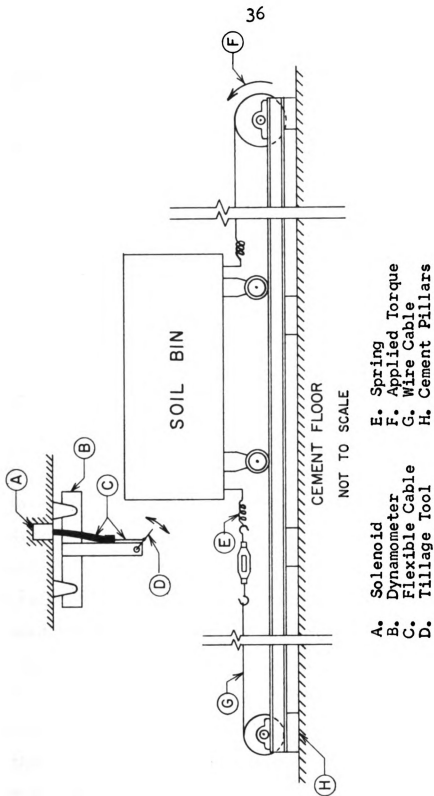


Figure 19. Schematic of the mobile soil bin and its related equipment.

shows a schematic of the most important parts of the bin and its related equipment.

The bin was 20 ft. long by 3 ft. wide by 12 in. deep. To catch soil which might be knocked out of the bin, movable gates were installed 2 ft. from either end and the center 16 ft. was filled with soil.

The bin was mounted on eight Rapistan Model 315OR-DURCH/TG wheels. The wheels rolled on 60 ft. long 3 in. "I" beam rails. The "I" beams were set on 5 in. by 5 in. cement pillars. The pillars were spaced on 5 ft. centers, and were constructed to provide a level base for the rails. Rubber pads were placed between the rails and the pillars to prevent vibrations in the rails from chipping the pillars. To fasten down the rails, $\frac{3}{8}$ in. threaded rods were screwed into lead screw anchors which were sunk into the original concrete floor. The rail pillars were then laid around the rods. A steel chip was put onto the threaded rod so that it overlapped the edge of the rail and a nut secured the chip to the pillar; the chip was then welded to the rail. To maintain constant spacing between the rails, 1-1/4 in. steel pipes were placed between the rails and $\frac{3}{8}$ in. rods were run through the pipes and through holes in the "I" beam rails. Nuts on the rods held the rails together, and the pipes prevented the rails from moving together.

The soil bin wheels were fitted with needle bearings and grease fittings. Each wheel had a load rating of 500 lbs.

To keep the soil bin on the rails, small steel guide wheels were mounted inside the rails and on the under side of the soil bin. The guide wheels rolled along the inside edge of the rails and were adjusted to allow a maximum of $1/8$ in. of lateral movement.

To provide movement and control for the soil bin, a flexible steel cable was connected to either end of the bin. The cable was attached to the bin through springs which allowed any sudden forces to be damped out. From the soil bin the cable ran over a free-running pulley mounted on one end of the rails and over a 6 in. diameter steel drum at the other end of the rails. The steel drum was connected to the power-take-off of a Massey-Ferguson 50 tractor. The power-take-off was run in the "Ground PTO" position, which allowed the use of the tractor transmission, clutch, brakes, and governor to control the soil bin speed and to decelerate the bin at the end of its run. The steel drum acted as a slip clutch to prevent excessive loads from being applied to the bin. The limiting factor in controlling the speed of the bin was found to be the tractor operator's ability to re-set the engine speed using the tachometer. An accuracy of ± 0.1 fps was achieved. The bin had a speed range of 0.75 fps to 4.0 fps, the maximum speed being limited by

the room available for starting and stopping. In the portion of the run in which the tool was in the soil the bin speed was found to be free of variation. Bin speeds of 1 fps, 2 fps, and 4 fps were used in the study. The bin speed was determined by "pips" spaced 1 ft. apart on the bin which actuated a micro-switch and caused 1 ft. intervals to be recorded by the oscillograph event markers.

In the event of failure of the soil bin stopping mechanism an arresting device was placed at the end of the rails. A large hook was mounted so as to engage the bin when it came within 4 ft. of the end of the rails. The hook was connected to a wire cable which was anchored to the cement floor by eight 1/2 in. bolts. A section of rubber bungee shock absorber was included in the arresting cable to help reduce the shock of an emergency stop.

Soil Conditioning Equipment.

In order to control the soil density, a method was devised to thoroughly mix and consolidate the soil between each series of tests.

The soil conditioning equipment, Figure 18, consisted of a rotary tiller (Roticul De-Lux) which was used to break and mix the soil after each series of tests. A series of Brillion 4C-533 packer wheels were used to reconsolidate the soil.

The soil was run beneath the rotating rotary tiller three times to insure complete break-up and mixing of the

soil. The loosened soil was then leveled by a leveling blade, and the packer wheels were lowered onto the soil. The soil bin was then moved back and forth while the packer wheels consolidated the soil. The number of times the packer wheels were run over the soil surface determined the soil density. After every second packing trip the packer wheels were moved half a packer-wheel width to either side, so that the soil compaction would be more uniform, and not consolidated in strips directly under each packer wheel. Next, a smooth steel roller weighted with water was lowered onto the soil surface and the bin was moved back and forth to smooth and consolidate the top layer of soil.

Tests were run at two soil moisture contents and two bulk densities at each moisture: (1) 14.0 % moisture content ± 0.6 %, bulk densities of 1.12 ± 0.02 gm/cc and 1.23 ± 0.03 gm/cc, (2) 17.5 % moisture ± 0.3 %, bulk densities of 1.12 ± 0.01 gm/cc and $1.23 \pm .01$ gm/cc.

To maintain the soil moisture, water was added at the end of each day's tests. The moisture was found to be constant within ± 0.35 % over a day's time. A polyethelene plastic cover was stretched over the soil surface whenever the tests were not in progress.

The soil cohesion and internal angle of friction were measured with a Bevameter (Figure 20). The Bevameter was built and loaned to Michigan State University by the Land Locomotion Laboratory, U. S. Army. The cohesion and inter-

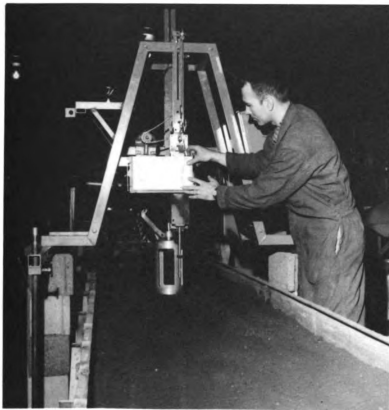


Figure 20. Bevameter used to measure soil parameters.



Figure 21. General view of recording equipment.

nal angle of friction both increased with increases in bulk density and moisture content. Figures 22 and 23 show results of the shear tests using the Bevameter. Table 13 presents data obtained using the Bevameter penetrometers.

Since the Bevameter shear head operated only on the top layer of soil the values obtained for cohesion and internal angle of friction do not necessarily reflect the values for the total depth of soil studied. However, these values do allow some comparison to be made of the soil parameters for each bulk density and moisture.

Analog Computer.

The oscillograph trace of the tool draft was readable when a rigid tool or the low frequencies of the vibrating tool were used. When the vibrational frequency was increased, however, the oscillograph trace was difficult to follow. To improve the accuracy of data evaluation an analog computer was used to integrate the varying draft force and to give the average draft force over each half-second period. Thus, the average draft for any tool frequency was obtainable.

Figure 24 is a schematic of the method used when employing the computer. The draft signal was fed into the strain gage amplifier. From the "Demodulator" connection on the amplifier the signal was fed into the "Vertical Axis Input" of a Tektronix model 532 oscilloscope, and amplified by the oscilloscope. The amplified signal was then taken

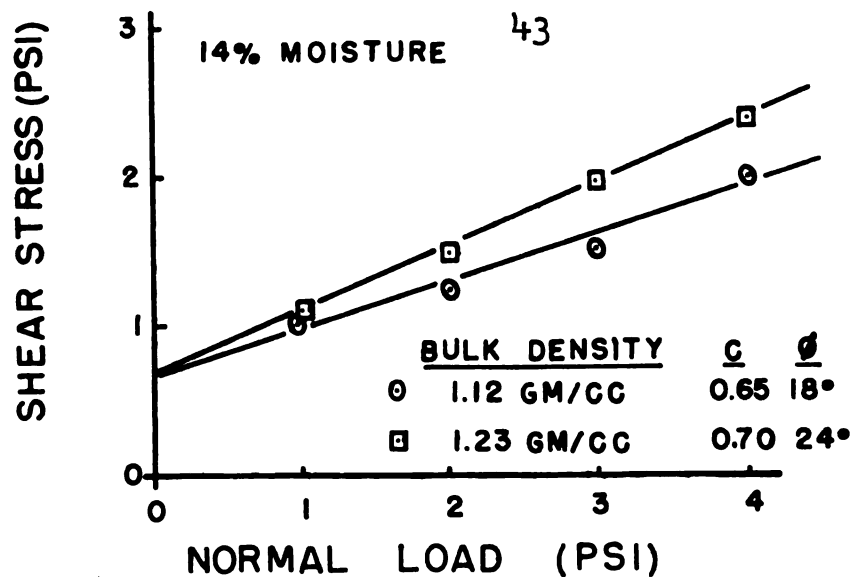


Figure 22. Soil parameters " c " and "Internal angle of friction" for soil at 14 % moisture and bulk densities of 1.12 and 1.23.

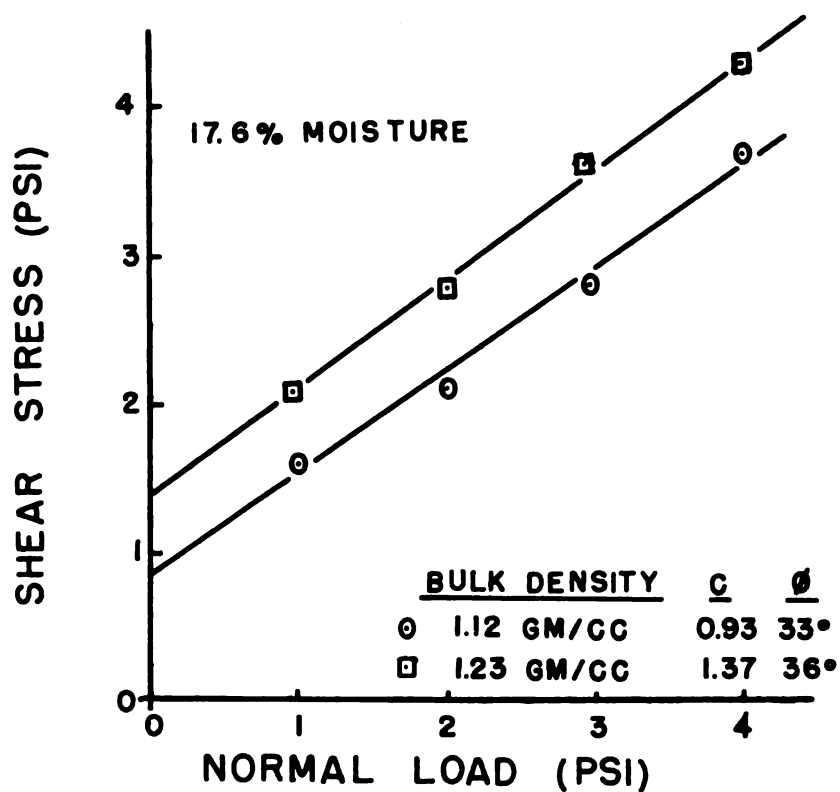
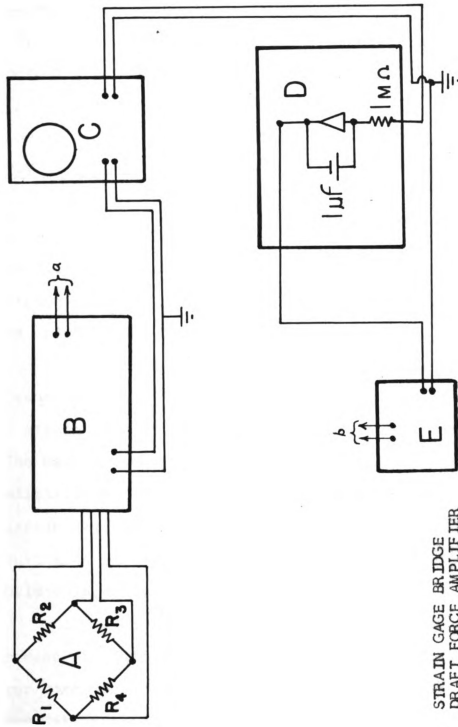


Figure 23. Soil parameters " c " and "Internal angle of friction" for soil at 17.5 % moisture and bulk densities of 1.12 and 1.23.



4

- A. STRAIN GAGE BRIDGE
- B. DRAFT FORCE AMPLIFIER
- C. OSCILLOSCOPE
- D. ANALOG COMPUTER
- E. DC AMPLIFIER
- a. TO DRAFT FORCE RECORDER
- b. TO RECORDER

Figure 24. Wiring schematic for recording the integrated draft signal.

from the "Vertical Axis Output" of the oscilloscope and fed into the Heathkit model EC-1 analog computer. The integrated signal from the computer was then put into the "DC Input" of another amplifier, and then from the amplifier the signal was recorded by the oscillograph. This method permitted simultaneously the recording of the instantaneous draft force, observing the oscilloscope trace of the draft force, and the integrated average draft force.

X-Y Plotter.

The X-Y recorder is a device which can record two variables simultaneously, one as a function of the other, on rectilinear coordinate paper. The recorder also has a calibrated time base on the X axis so that one variable can be recorded as a function of time.

In order to record any variable, the signal from the transducer must be converted into a DC voltage signal; i.e., a strain gage bridge output, a thermocouple voltage, etc. The maximum sensitivity of the Mosley 135 plotter is 0.5 millivolt per inch deflection. Therefore, with a 4-arm strain gage bridge, a stress in steel of 10,000 psi will result in a pen deflection of approximately 10 in. with a bridge input of 6 volts.

Figure 25 is a picture of the X-Y plotter and two pieces of equipment which were constructed to make the plotter more versatile. Figure 25 B is the Strain Gage Balance and Calibration Unit, designed and constructed by the author from information provided by the Detroit Arsenal, Land

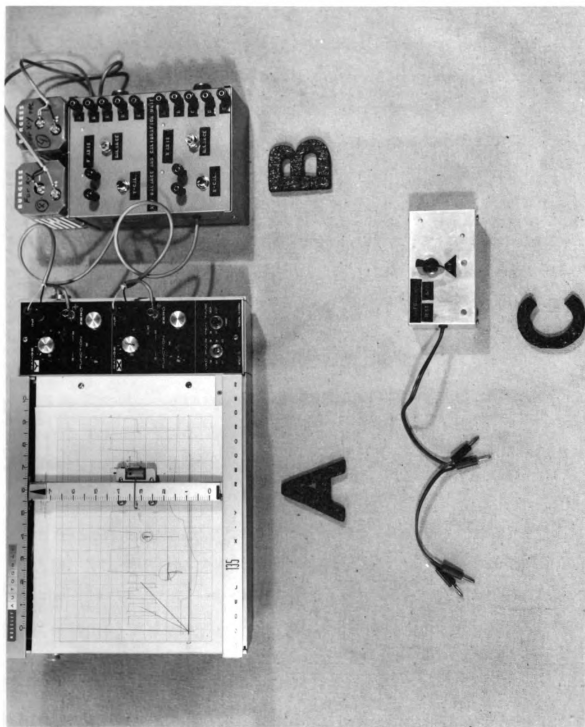


Figure 25. Mosley X-Y Plotter (A), Strain Gage Balance and Calibration Unit (B), and Performance Test Rig (C).

Locomotion Laboratory, U. S. Army. The Strain Gage Balance and Calibration Unit allows the plotter to be used directly with a strain gage bridge without an external amplifier, and is essentially equivalent to the strain gage input box of the Brush universal amplifier, except that no method for capacitance balance was included. The input to the Strain Gage Balance and Calibration Unit was designed in order that a number of methods of connection could be used. The input connections are 5-way binding posts and female Amphenol fittings. The wiring diagrams of the Amphenol fittings and the binding posts are the same as the Brush universal amplifier; the connectors used for the plotter can be used on other strain gage equipment. Figure 26 is the wiring diagram for the Strain Gage Balance and Calibration Unit.

Figure 24 C is the Performance Test Rig for the X-Y plotter, as outlined in the Mosley instruction manual. Figure 27 is the wiring diagram of the Performance Test Rig. This device can be used to test the performance of both axes of the plotter simultaneously and any irregularities in the resultant trace will indicate a malfunction in the operation of either axis. A page in the instruction manual points out specific malfunctions, how they will look, and how to rectify them.

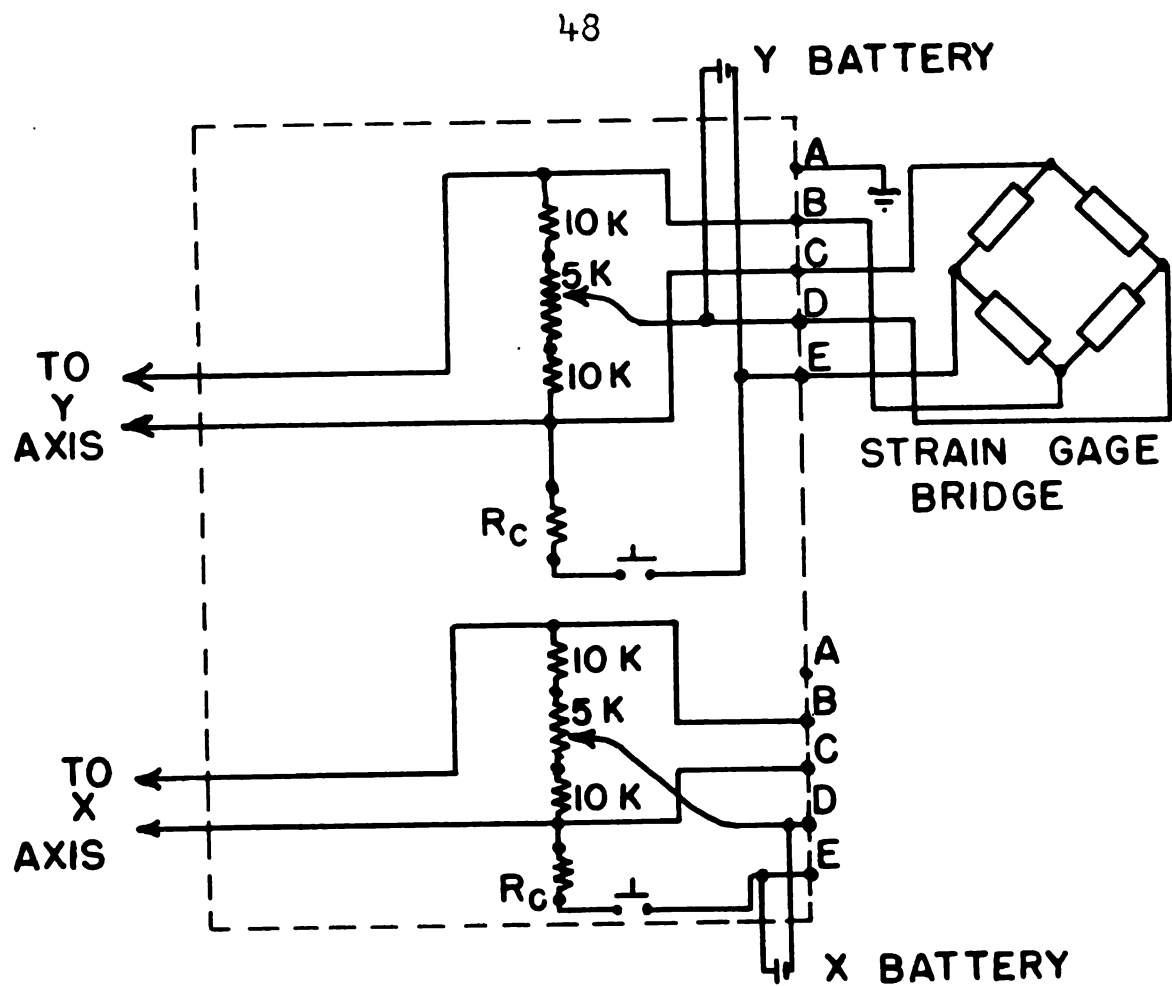


Figure 26. Strain Gage Balance and Calibration Unit wiring diagram.

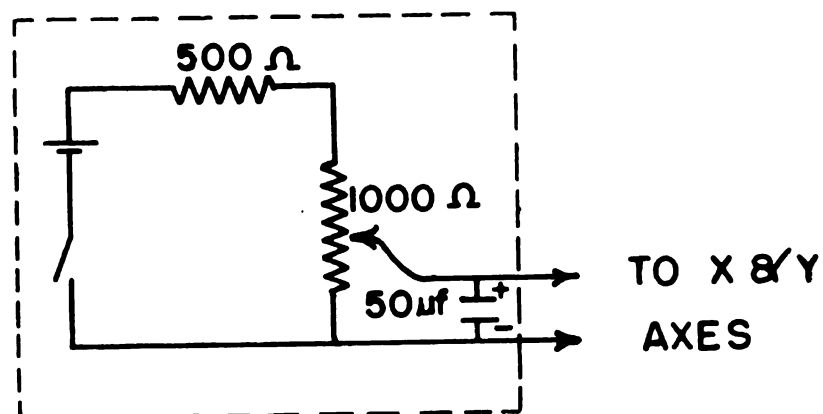


Figure 27. Performance Test Rig wiring diagram.

THEORETICAL CONSIDERATIONS

Calculation of the Draft Force on a Rigid Tool.

Soehne (1956) presented the following equation for the horizontal resistance (draft) of an inclined plane moving through the soil:

$$F_x = N_o (\sin \delta + \mu'_o \cos \delta) + kb$$

where: F_x = Draft force (lb.)

N_o = Force acting normal to the plane (lb.)

δ = Angle of inclination of the plane to the horizontal (degrees)

k = Width of the soil slice (in.)

b = Unit resistance of the soil to being cut by the plane edge (lb. per in.)

μ'_o = Apparent coefficient of friction of the soil on the plane surface

Prior to this time there has been no satisfactory method of confirming the theoretical analysis by laboratory tests since the individual values could not be measured separately. Soehne states that, "Agreement between the calculated and measured values is not particularly good". With the equipment employed in this investigation, however, all the individual components were separated and measured. F_x was measured directly, and δ was held fixed. A close estimate of N_o could be made from the pressure cells installed on the face of the tool, and kb was measured by simulating the cutting action of the plane edge by substituting a wire for the tool. μ'_o was determined from a series of tests.

To confirm the theoretical equation, a series of calculations was made from data gathered on a tool at an angle of inclination $\delta = 40^\circ$, soil moisture 17.5 %, bulk density 1.23 gm/cc, and a forward velocity of 2.0 fps.

From the coefficient of friction tests, the value of μ'_0 was found to be 0.48 for the first 1/4 in. of the tool (steel), and 0.31 for the remainder of the surface (Teflon). A value of $k_b = 15.5$ lb. was determined from the tests using a wire to represent the cutting edge.

An average value for N_{OT} for the Teflon-covered portion of the tool was calculated from the measured normal forces by the following procedure:

1. The average pressure across the tool was calculated from the pressures indicated by cell nos. 2, 4, and 5.
2. The average pressure acting across the tool was divided by the pressure indicated by cell no. 2 to obtain the pressure distribution across the plane (pressure distribution coefficient, q).
3. The recorded pressures of cell nos. 1, 2, and 3 were averaged to obtain the average normal pressure distribution along the longitudinal centerline of the plane.
4. The averages of cells 1, 2, and 3 were then multiplied by the pressure distribution coefficient, q , which resulted in an overall average value for

the unit pressure. The unit pressure was then multiplied by the Teflon-coated area to obtain the value for N_{OT} .

The value for the average normal pressure acting on the steel edge of the tool (N_{Os}) was determined from the product of the pressure recorded by cell no. 1 and the coefficient, q . The calculated value was smaller than the actual normal pressure. It is, however, the best information available and must be used until a method can be developed to measure normal pressure on a very narrow strip of material.

The theoretical draft equation for a tool consisting of two different surface materials is as follows:

$$F_x = N_{OT}(\sin \delta + \mu'_T \cos \delta) + N_{Os}(\sin \delta + \mu'_s \cos \delta) + kb$$

The calculated values for F_x and the measured value for F_x are shown in Table 11. The letter "M" following the test number indicates that the maximum recorded forces were used in the calculation and the letter "A" indicates that the average recorded forces were used. The average value for the ratio of calculated draft to the measured draft was found to be 0.91. A better agreement could probably be obtained by using an actual measured value for the normal force acting on a steel edge.

Discussion of Draft Reduction by a Vibrating Tillage Tool.

By considering each of the forces acting on a rigid tillage tool separately, one can determine which forces

would be increased or decreased by the use of vibrating energy.

The force due to the apparent coefficient of friction and normal force ($\mu' N_0$ in Figure 2) would be increased during the portion of the cycle in which soil was being accelerated upward. Immediately following the upward movement, soil would be lifted upward and exert little or no normal force for a short period of time, and then fall back onto the tool surface in a loosened condition. Forcing the tool into the soil at a more acute angle (in the plane of the tool) would reduce the "bulldozing" effect and reduce the value of N_0 .

The cutting force (S) would be reduced only in the case where the leading edge of the tool was not actively cutting into new soil during a portion of the time, as in the case of Eggenmueller's and Gunn's experiments.

Resistance to shear plane formation ($cF + \mu_1 N_1$) could be decreased by reducing either the soil cohesion (c) or the normal force acting upon the shear plane (N_1). The area of the shear plane (F) and the internal coefficient of friction (μ_1) appear to be fixed for any one tool and soil type. No practical method of reducing cohesion is known. However, under rapid loading rates there is evidence to indicate that the total strain energy required to overcome the cohesive force is reduced (Hendrick, 1960). Thus, a mode of vibration in which the shear plane is formed very

rapidly would result in less strain energy required to form each shear plane.

The author observed during Harris's (1961) research (in which a plate was forced downward upon soil in a container while recording the resulting internal soil stresses) that regardless of the amount of normal force applied, and regardless of the initial deformation of the soil surface, a very slight reduction in applied force resulted in a corresponding reduction in soil internal stress. After an initial soil deformation of as much as 2 in., if the applied force was reduced to zero, the internal soil stress reduced to zero also, even when the rebound of the loading plate was negligible. Thus, if the mode of vibration of a tillage tool were such that the tool tip moved at an angle of more than 90° to the angle of shear plane formation, any normal force (N_1) acting on the soil shear plane would be reduced, causing a resulting reduction in the shearing resistance. No method is available to measure this force under operating conditions.

Forces due to soil acceleration (A) during the vibrating cycle would be greatly increased during the lifting portion of the tool movement, depending upon the acceleration imparted to the tool. A small accelerating force would also act as the tool moved forward into new soil.

The force due to the soil weight (G) would act any time the soil was on the tool surface. This force could be

reduced by making the tool short to reduce the soil supported by the tool at any instant.

RESULTS

Simulation of Cutting Resistance.

In order to determine the portion of the total force due to the cutting action of the leading edge of the tool, a wire was substituted for the tillage tool and run through the soil at the depth of the tool edge. Two diameters of wire were used: 0.008 in. and 0.041 in. The 0.041 in. diameter wire closely matched the thickness of the cutting edge of the instrumented tool, and the 0.008 in. diameter wire matched the cutting edge of the second tool.

Figure 28 illustrates the horizontal force due to the cutting action of the two wires in relation to the cutting velocity at 17.5 % moisture and the two bulk densities used in the tillage tool tests. An interesting result was the small increase in cutting resistance as the velocity was increased. A similar result was obtained in tests at the National Tillage Machinery Laboratory (1961). The average force increased 9 % with a velocity increase of from 1 ft. per sec. to 4 ft. per sec. When the wire was run a second time in the same cut, the force was 0.47 that of the original force. At the lower bulk density the ratio of average cutting force of a wire to total draft of the rigid tool was 0.54; at the higher density the ratio was found to be 0.56.

Thus, any mode of operation in which the cutting edge of the tool moves into the soil only a portion of the time

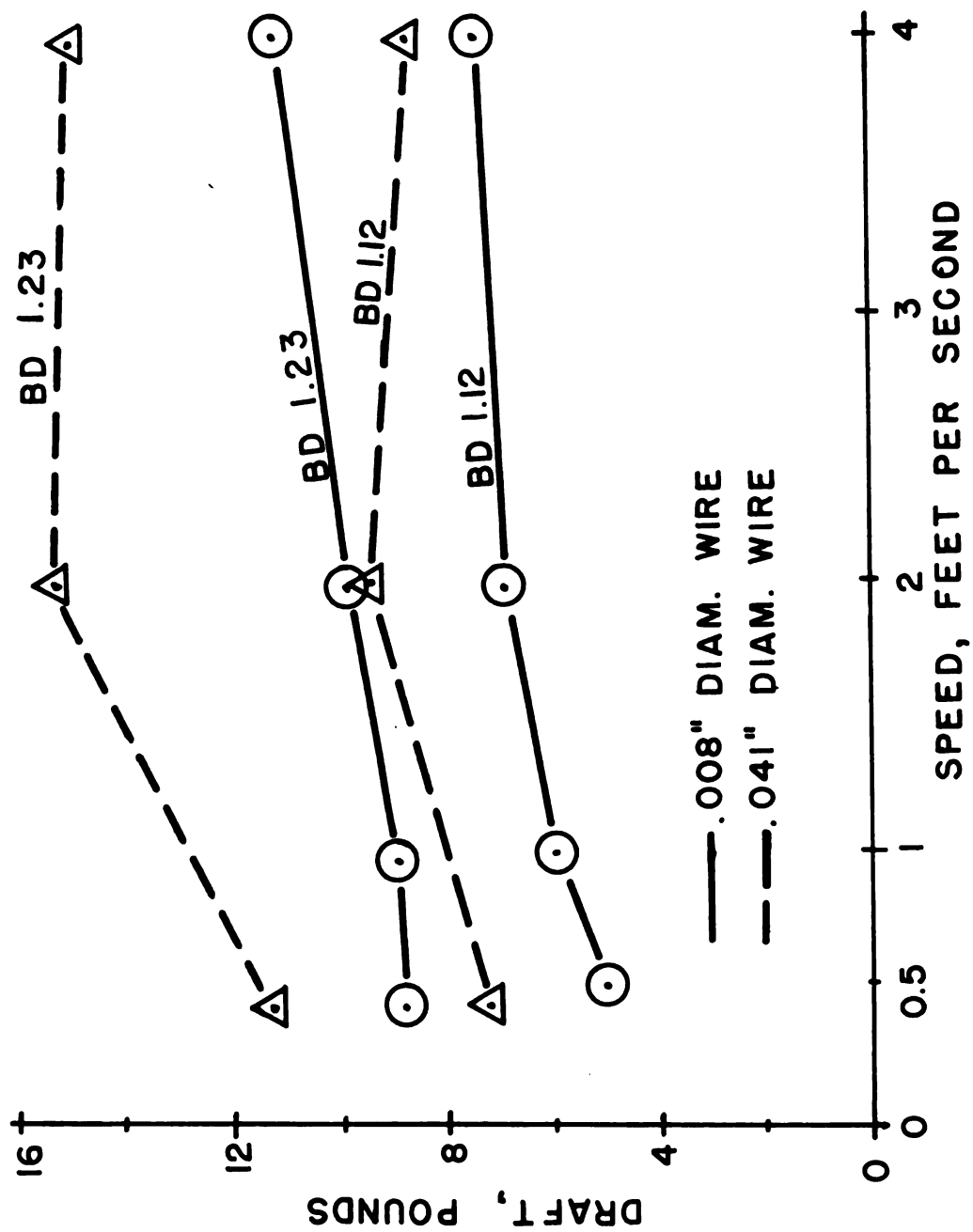


Figure 28. Horizontal force of cutting for two wires as a function of velocity.

would result in a considerable reduction in the cutting force. In the modes of vibration employed by both Eggenmueller and Gunn the tool did not cut forward into new soil during a portion of the operating cycle.

Reduction of Draft Force.

The draft ratio (ratio of the average draft of a vibrating tool to the average draft of a rigid tool: D_v/D_a) was less than one for all but 5 of the 154 tests conducted.

Figures 29, 30, and 31 are graphs of draft ratio versus cycles per foot in experiments run at a working angle (δ) of 40° at 10° , 15° , and 20° displacement angles (angles the blade was rotated by the solenoid) and in soils at 14 % moisture and 17.5 % moisture. Each point is the average of 4 replications. The notation $40^\circ/10^\circ$ represents a working angle (δ) of 40° and a displacement angle (γ) of 10° . Figures 32 and 33 illustrate the draft ratio as the angle of action was increased.

Figures 34, 35, 36, and 37 illustrate the decrease in the draft ratio in experiments run at a working angle of 30° and displacement angles of 5° , 10° , 15° , and 20° for soil moisture contents of 14 % and 17.5 %. Figures 38 and 39 illustrate the decrease in draft ratio as the displacement angle was increased.

The data for all tests are tabulated in Tables 7, 8, 9, and 10.

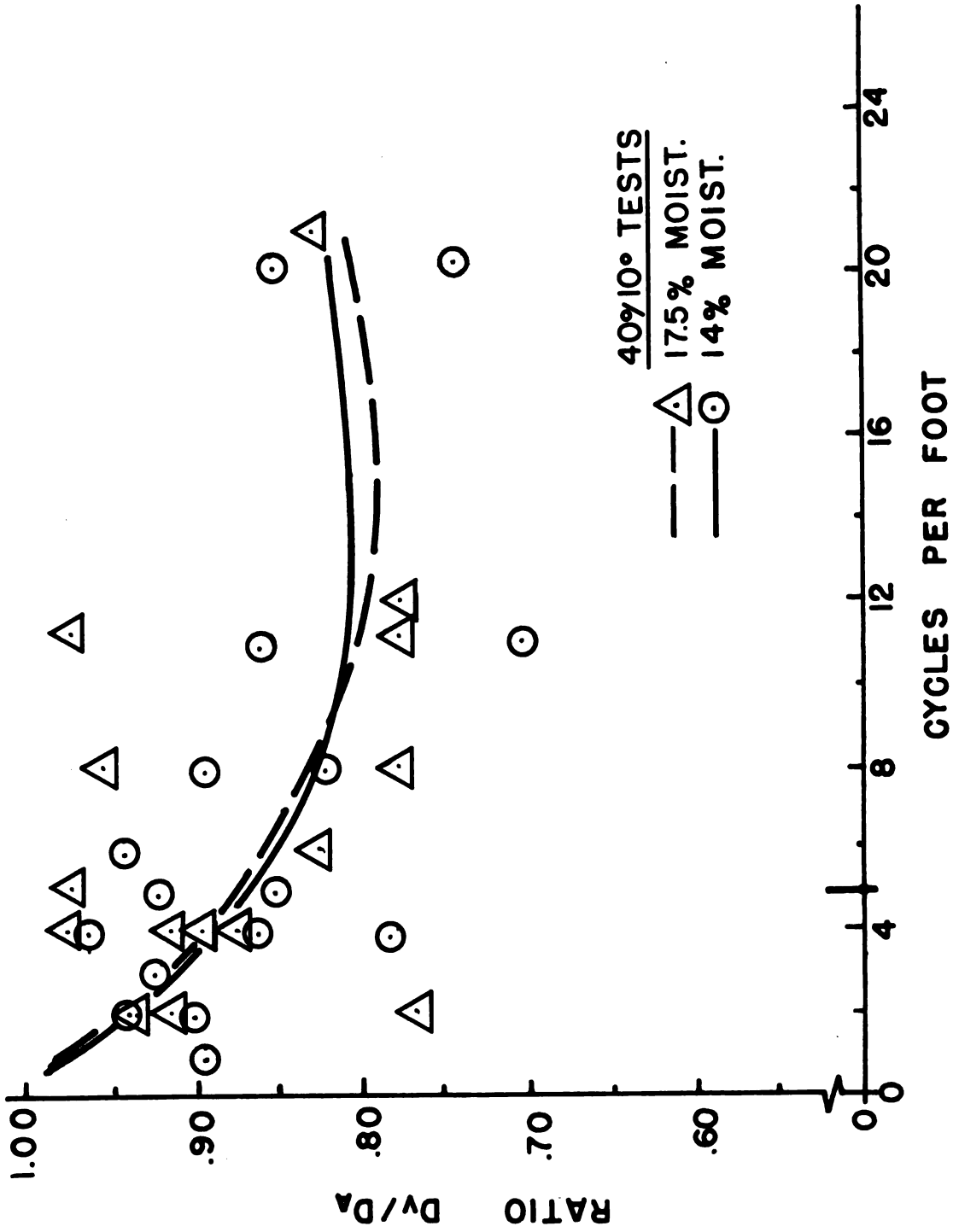


Figure 29. Draft ratios of a vibrating and rigid tool for $\delta = 40^\circ$ and $\delta = 10^\circ$.

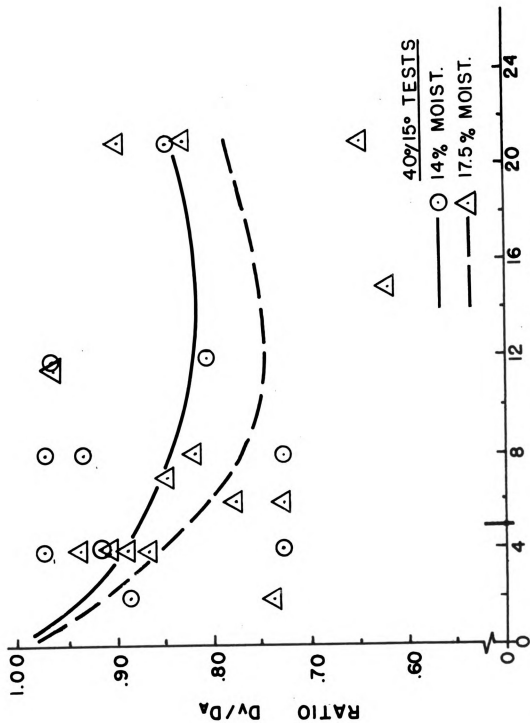


Figure 30. Draft ratios of a vibrating and rigid tool for $\phi = 40^\circ$ and $\delta = 15^\circ$.

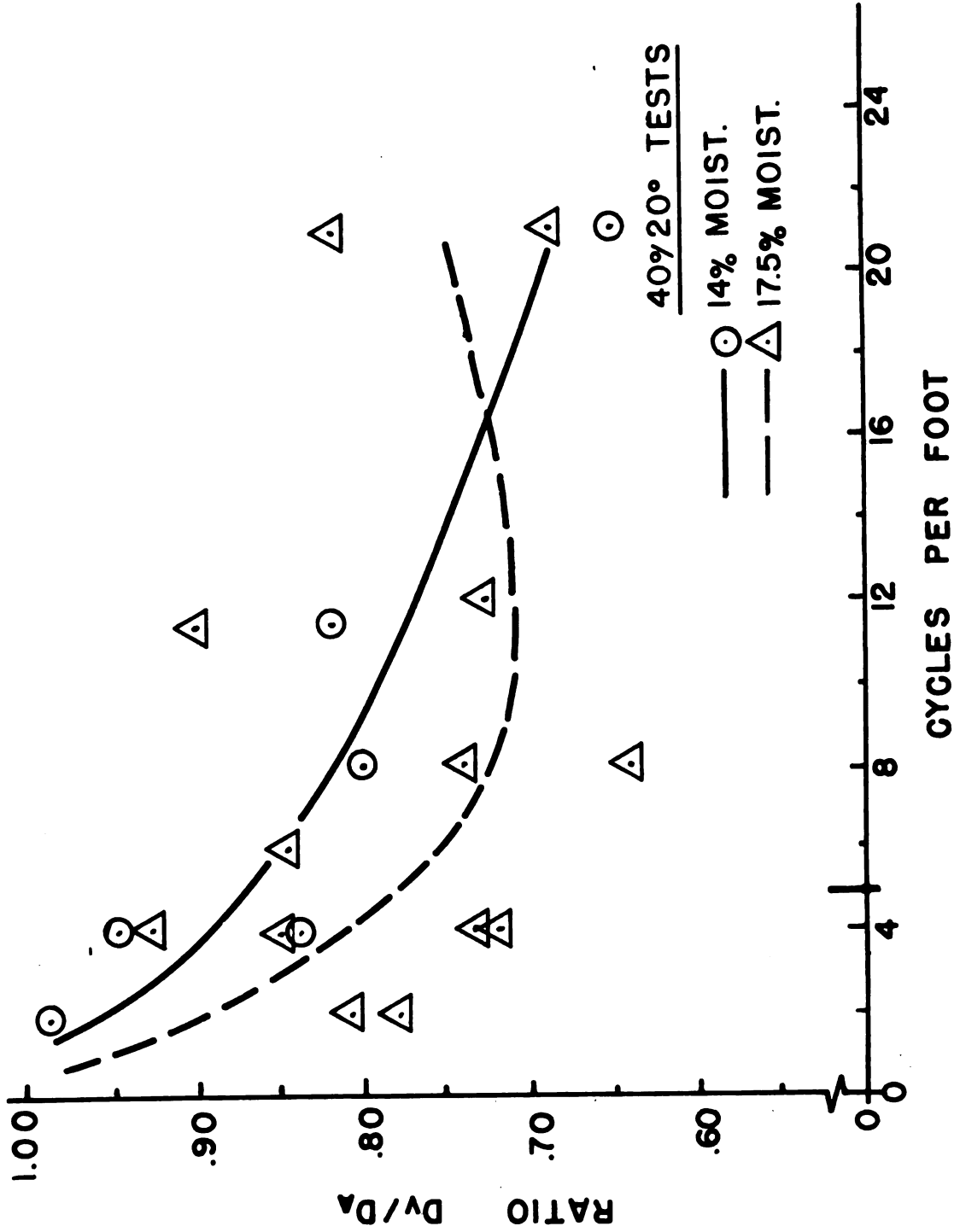
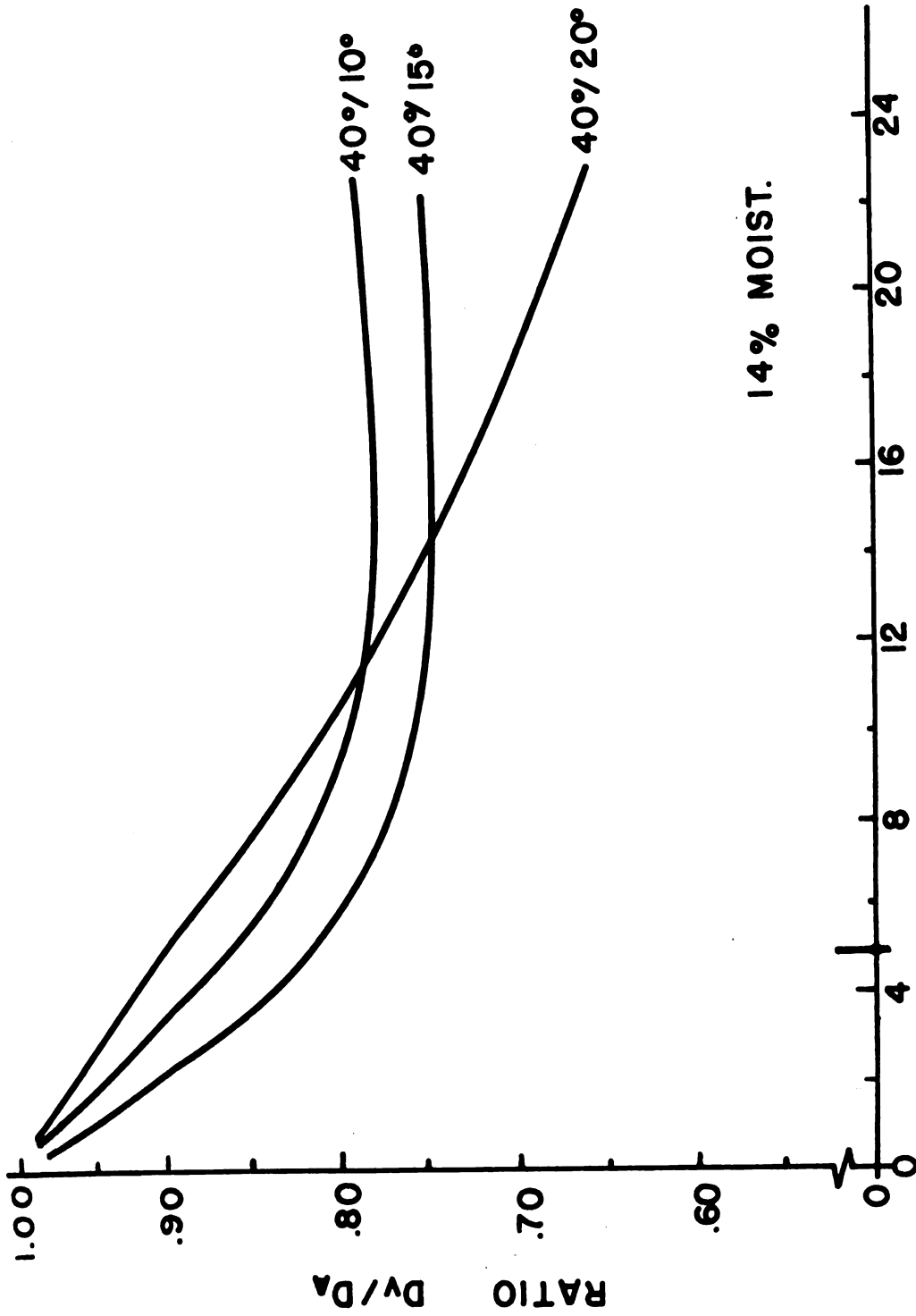


Figure 31. Draft ratios of a vibrating and rigid tool for $\delta = 40^\circ$ and $\beta = 20^\circ$.



CYCLES PER FOOT

Figure 32. Relation of draft ratios for $\delta = 40^\circ$ and $\delta = 10^\circ, 15^\circ$, and 20° at 14 % soil moisture.

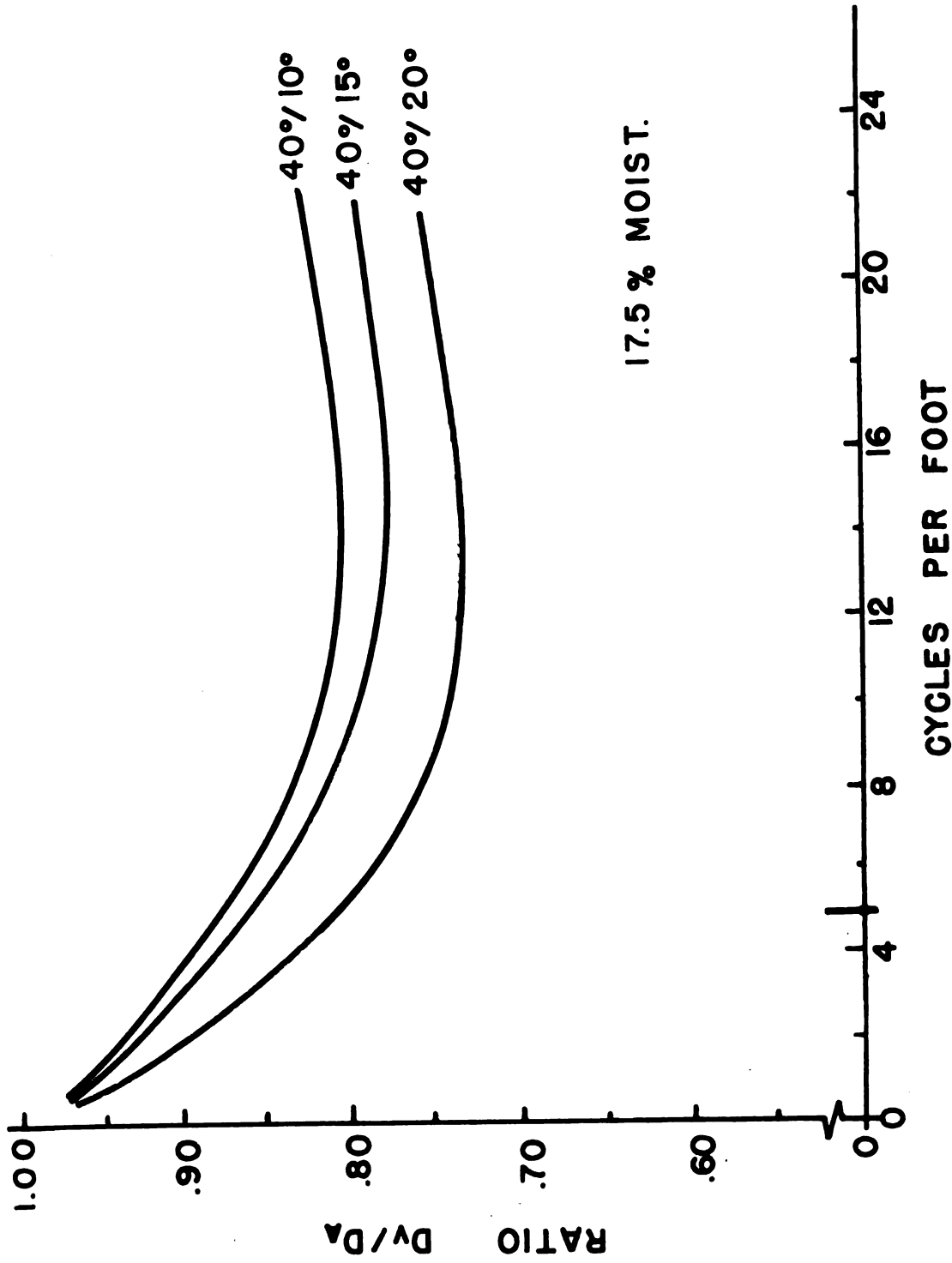


Figure 33. Relation of draft ratios for $\delta = 40^\circ$ and $\delta = 10^\circ, 15^\circ$, and 20° at 17.5 % soil moisture.

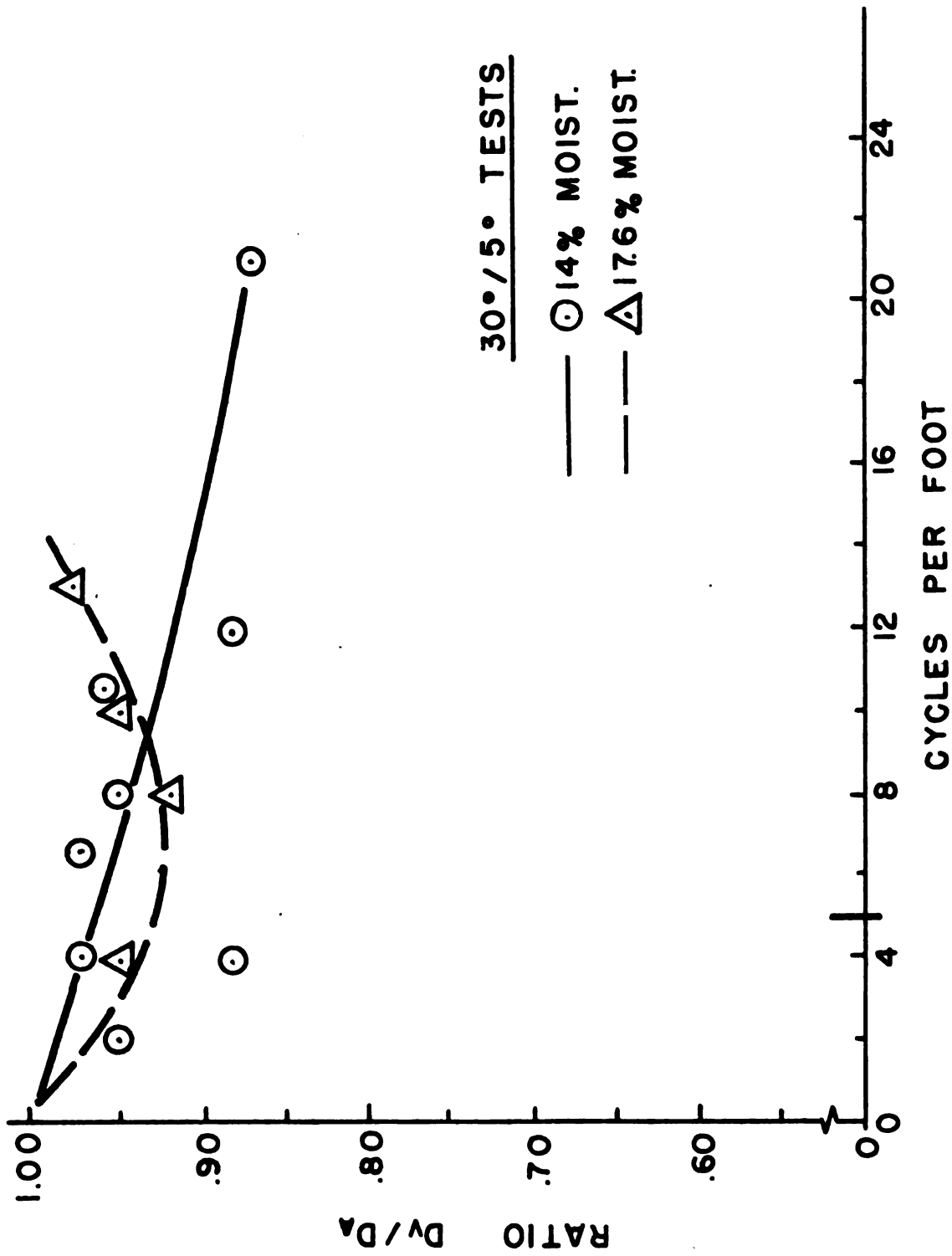


Figure 34. Draft ratios of a vibrating and rigid tool for $\delta = 30^\circ$ and $\gamma = 5^\circ$.

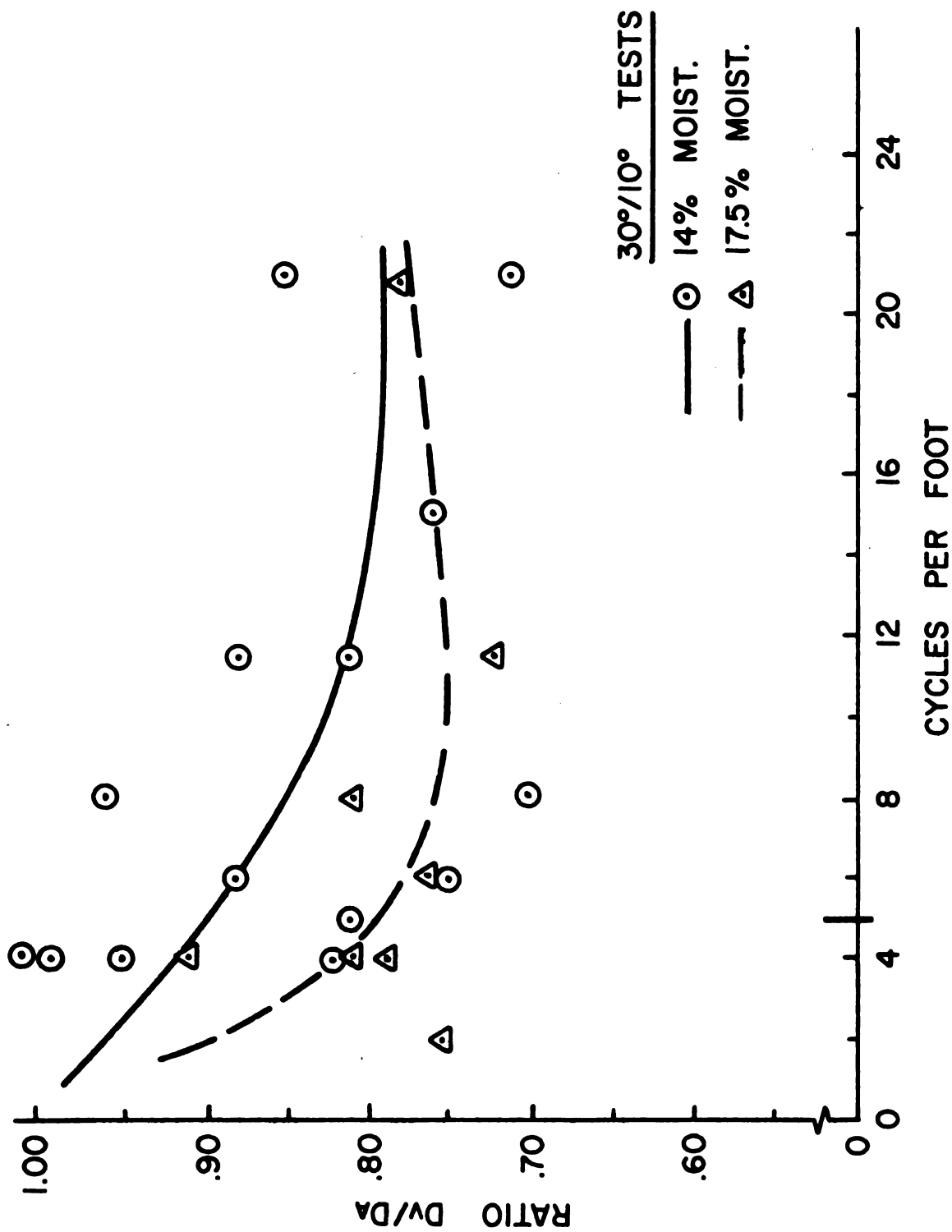


Figure 35. Draft ratios of a vibrating and rigid tool for $\delta = 30^\circ$ and $\gamma = 10^\circ$.

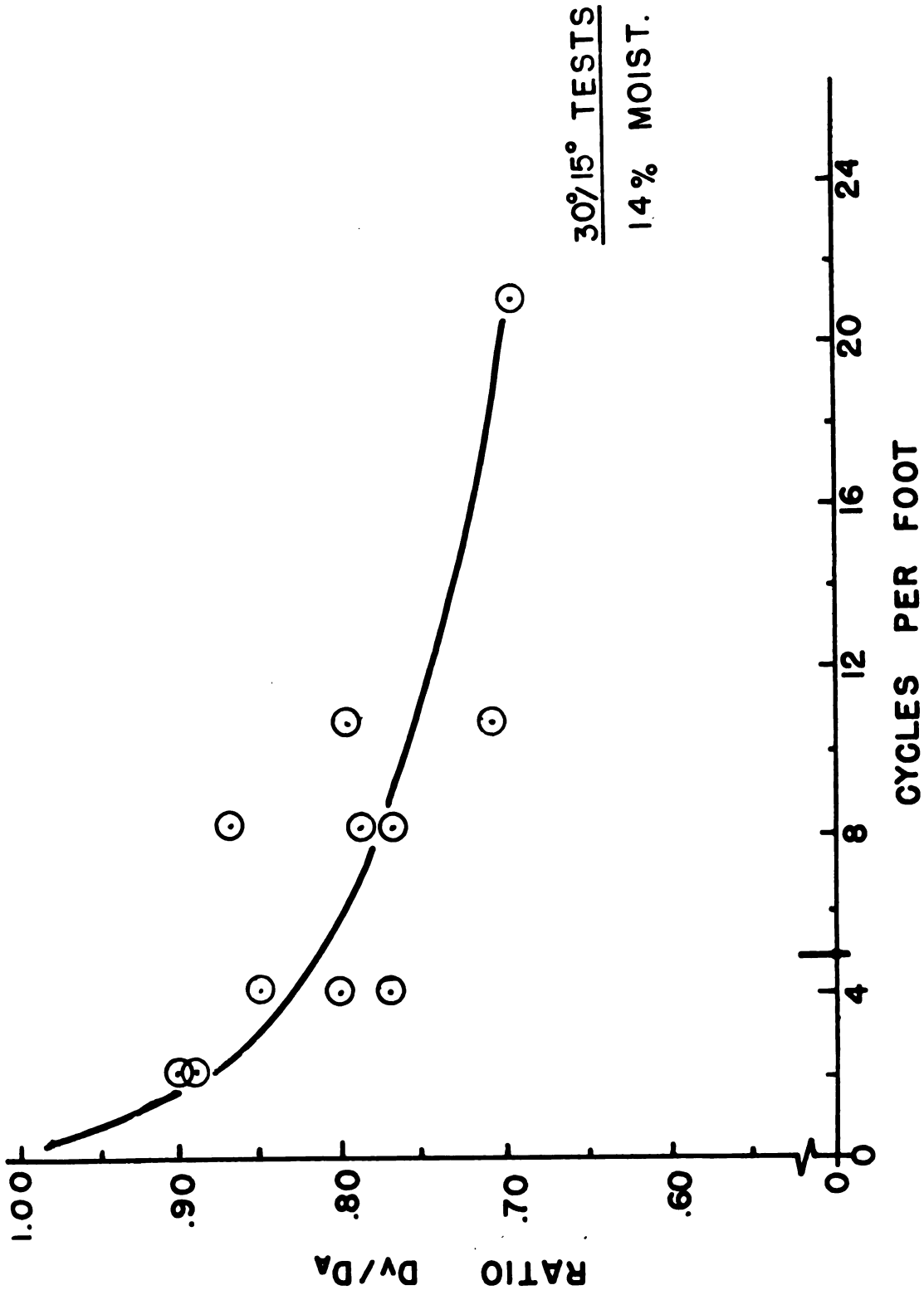


Figure 36. Draft ratios of a vibrating and rigid tool for $\delta = 30^\circ$ and $\gamma = 15^\circ$.

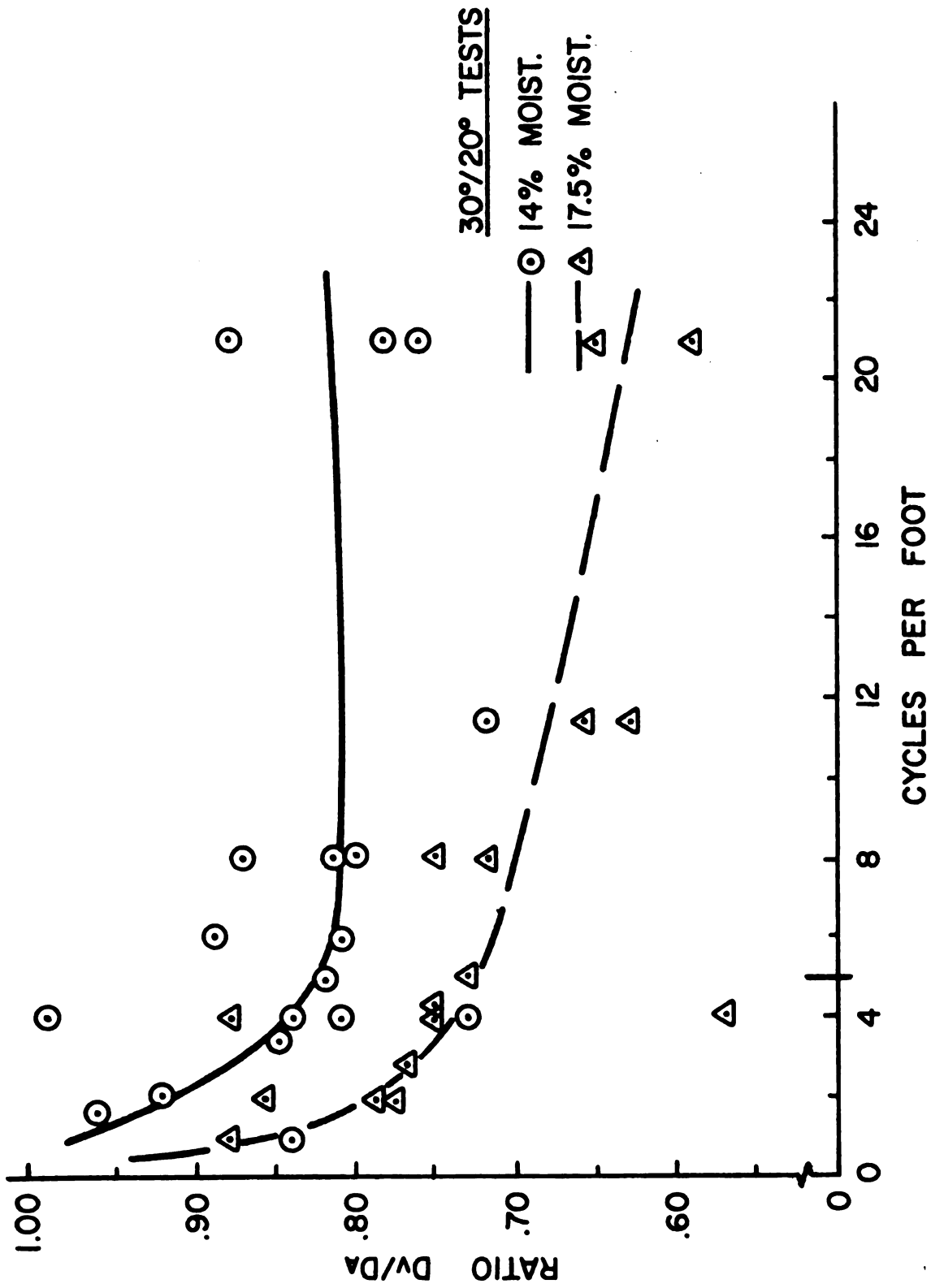


Figure 37. Draft ratios of a vibrating and rigid tool for $\delta = 30^\circ$ and $\gamma = 20^\circ$.

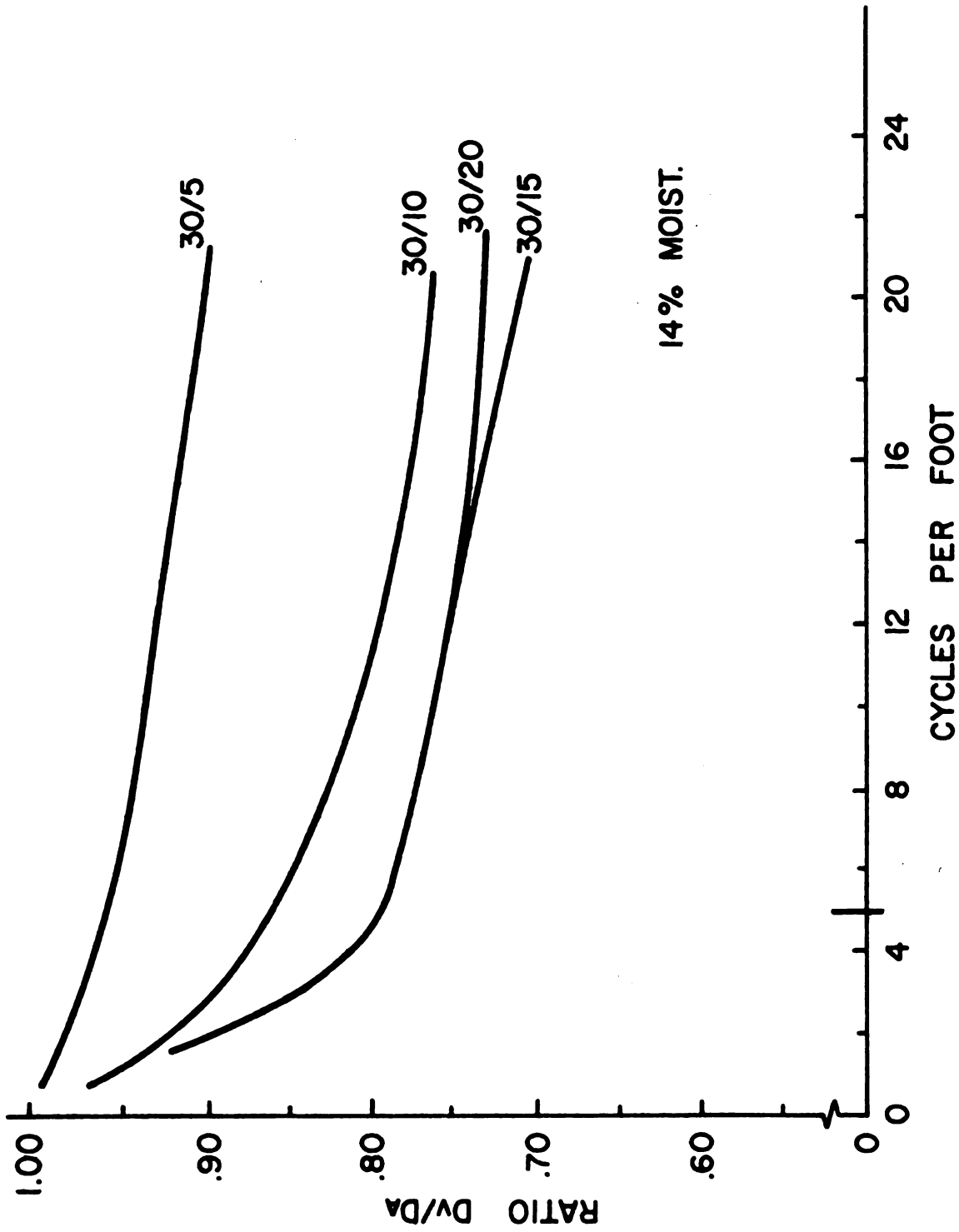


Figure 38. Relation of draft ratios for $\delta = 30^\circ$ and $\gamma = 5^\circ, 10^\circ, 15^\circ$, and 20° at 14 % soil moisture.

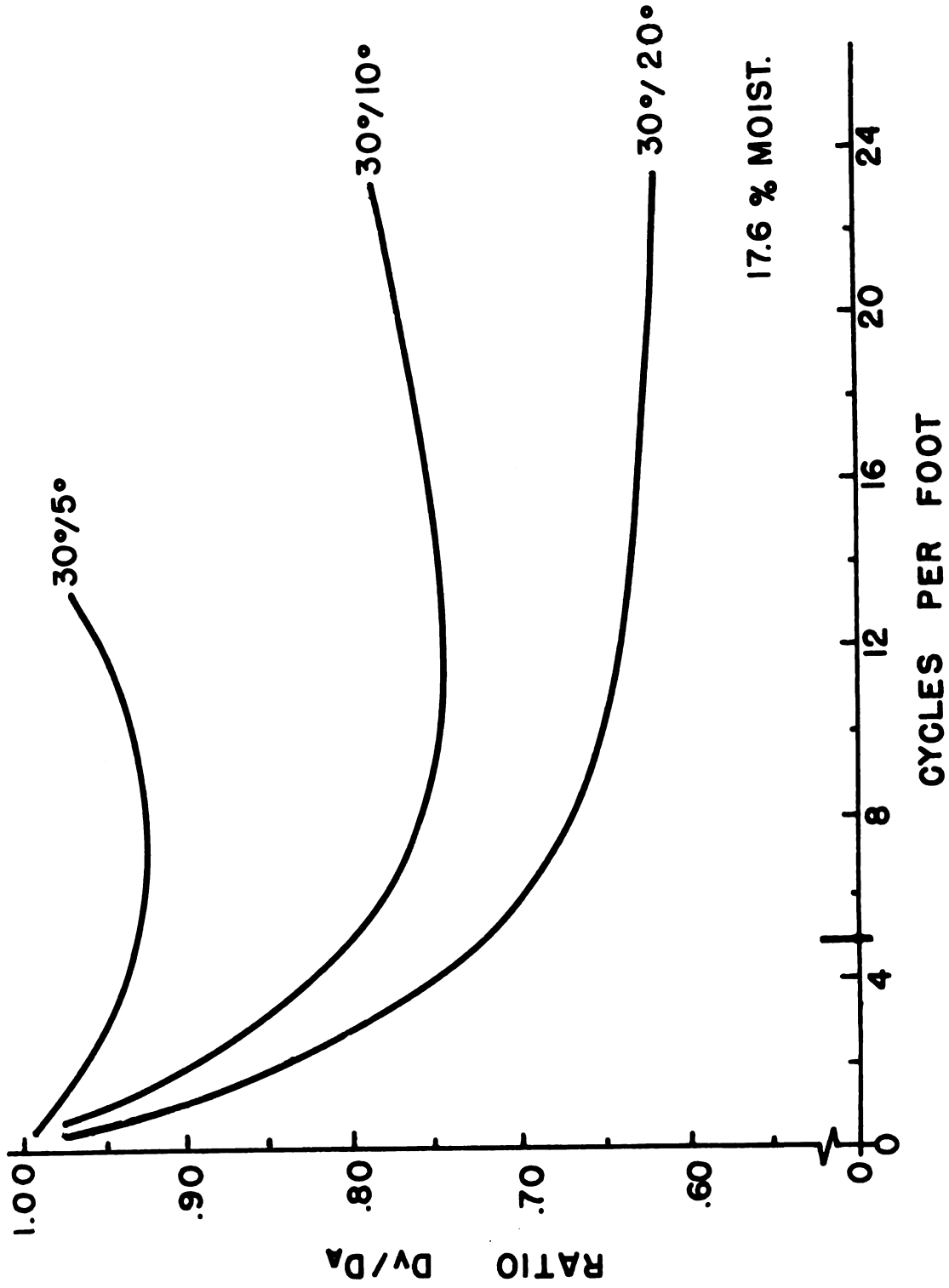


Figure 39. Relation of draft ratios for $\delta = 30^\circ$ and $\delta = 5^\circ, 10^\circ, 15^\circ$, and 20° at 17.5 % soil moisture.

An F test was made to test the hypothesis that the mean draft ratios were equal for experiments conducted at the same working angle and displacement angle but in 14 % and 17.5 % soil moistures for corresponding values of cycles per foot. The hypothesis was rejected at the .05 level of significance for all tests except the 40°/10° and 30°/5° experiments. From this it can be concluded that for at least one value of cycles per foot in each rejected test the reduction ratio was significantly less for the 17.5 % moisture tests than for the 14 % moisture tests. Closer observation of the data indicates that the draft ratio was generally lower at 17.5 % moisture than at 14 % moisture.

An F test was made to test the hypothesis that the mean draft ratio was equal for experiments conducted at different displacement angles but at the same working angle and soil moisture. The hypothesis was rejected at the .05 level of significance for all but the 30°/15° vs. 30°/20° and 40°/15° vs. 40°/20° experiments. It can therefore be concluded that for at least one value of cycles per foot in each rejected test the reduction in draft was significantly greater for the larger displacement angle. Closer observation of the data indicates that in general a larger displacement angle reduced the draft ratio.

As may be expected, there was a tendency for the draft ratio of the tool run at a working angle of 30° to be less at each corresponding displacement angle than for tools

run at a working angle of 40° . This would appear to be due to either or both of two factors: (a) at the 30° working angle the tool tip moved upward at an angle at or greater than 90° to the soil shear plane, which reduced the normal force (N_1) on the soil shear plane, and (b) a larger portion of the force transmitted by the solenoid acted in the horizontal direction when a working angle of 40° was used. Due to the design of the model tool, and from the results of the tests conducted to determine the forces the solenoid exerted upon the tool, the second factor can be neglected since the point of attachment between the flexible cable and the tool resulted in a smaller moment being exerted upon the tool at a 40° working angle at a specified solenoid force, and since the force exerted upon the tool by the solenoid was virtually the same for both 30° and 40° working angles.

The greater reduction in draft force at an angle of 30° was, therefore, probably due to a reduction of N_1 , since the tool tip did move at an angle greater than 90° to the shear plane. The soil shear planes created by the tillage tool were observed to have an angle of 28° to 30° with the soil surface. Unfortunately, there is no reliable method available for measuring the normal force acting on the shear plane.

By activating the tool tip upward, the applied force was more nearly parallel to the direction of the soil shear

plane and soil displacement; this resulted in a more efficient application of the tillage forces.

Energy Requirement of the Vibrating Blade.

A comprehensive analysis of the soil forces during operation of the vibrating tillage tool is not possible at the present time. Many of the variables which must be considered cannot be measured, or even estimated with any degree of accuracy.

The normal force acting upon the soil shear plane (N_1) cannot be measured, even though the reduction of that force is one of the possible advantages of a vibrating blade.

Another soil force, the cohesion acting on the soil shear plane, cannot be measured under extreme loading rates. The reduction of total strain energy by reducing the displacement required to cause failure of the cohesive bonds by rapid loading was another possible advantage of the vibrating tillage tool. An observation was made, however, that when the blade was moved slowly (by hand) through an angle of 10° , a shear plane was not developed; when the blade was moved rapidly through the same arc by activating the solenoid a shear plane developed.

In a preliminary investigation to determine the acceleration of a soil slice by the vibrating blade, the vertical displacement of a rigid body placed on the blade at the point of percussion and accelerated by the action of the blade was calculated. If the blade was at a working angle

(8) of 40° and activated by the solenoid through an angle of 10° , the rigid body would have been displaced a total distance of 1.1 in. in the vertical direction. Since the observed vertical displacement of the soil slice was less than half an inch, the remaining displacement and energy must have been absorbed in shattering and compacting the soil on or near the tool face.

The only remaining method of determining the energy requirement was to measure the energy applied to the soil by the combination of draft force and solenoid action. The input energy due to the draft force was simply the product of average draft force times unit distance. The input energy due to the solenoid was calculated from the solenoid movement, the force applied to the blade, and the frequency of operation. Table 6 lists the solenoid energy input to activate: (1) the blade alone, (2) the blade and loose soil, and (3) the blade in forming a new shear plane for one cycle.

In order to determine the energy the vibrating blade applied to the soil compared with the energy requirement of a rigid blade, the draft of a rigid blade per unit of travel was considered as 100 %. The relative draft of the vibrating tool was then one energy input, and the energy of the solenoid was the other input (the solenoid energy required to accelerate the blade alone was subtracted from the total solenoid energy since it was not actually applied

to the soil). Figures 40 through 44 illustrate the comparative energy input to a vibrating tool under various conditions of working angle and displacement angle as a function of the number of cycles per foot of travel.

In general, the energy requirement of the vibrating tool was observed to be less than that of the rigid tool for a narrow range of low frequencies; it then exceeded the energy requirement of a rigid tool. It should be noted, however, that at the higher vibrational frequencies (10 to 15 cycles per foot of travel) more shear planes were formed per unit distance traveled by the vibrating tool than by the rigid tool, resulting in better particle size reduction. The shear plane formation of the rigid tool was very nearly constant at 5 shear planes per foot. At frequencies above 15 cpf, the blade did not return to its maximum working angle before it was activated again, which resulted in its operating through a smaller displacement angle during each cycle; therefore, it did not form distinct shear planes. That condition was observed during the analysis of the recorded forces; when frequencies above 15 cpf were used, the rigid-tool pattern of shear plane formation was recorded with small forces superimposed upon them each time the solenoid was actuated.

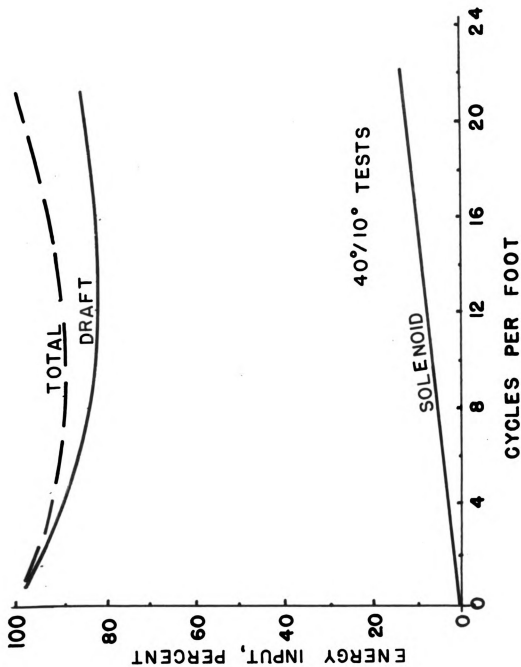


Figure 40. Percent energy applied by draft and solenoid action of a vibrating tool compared to a rigid tool where $\delta = 40^\circ$ and $\rho = 10^\circ$ at 17.5% soil moisture.

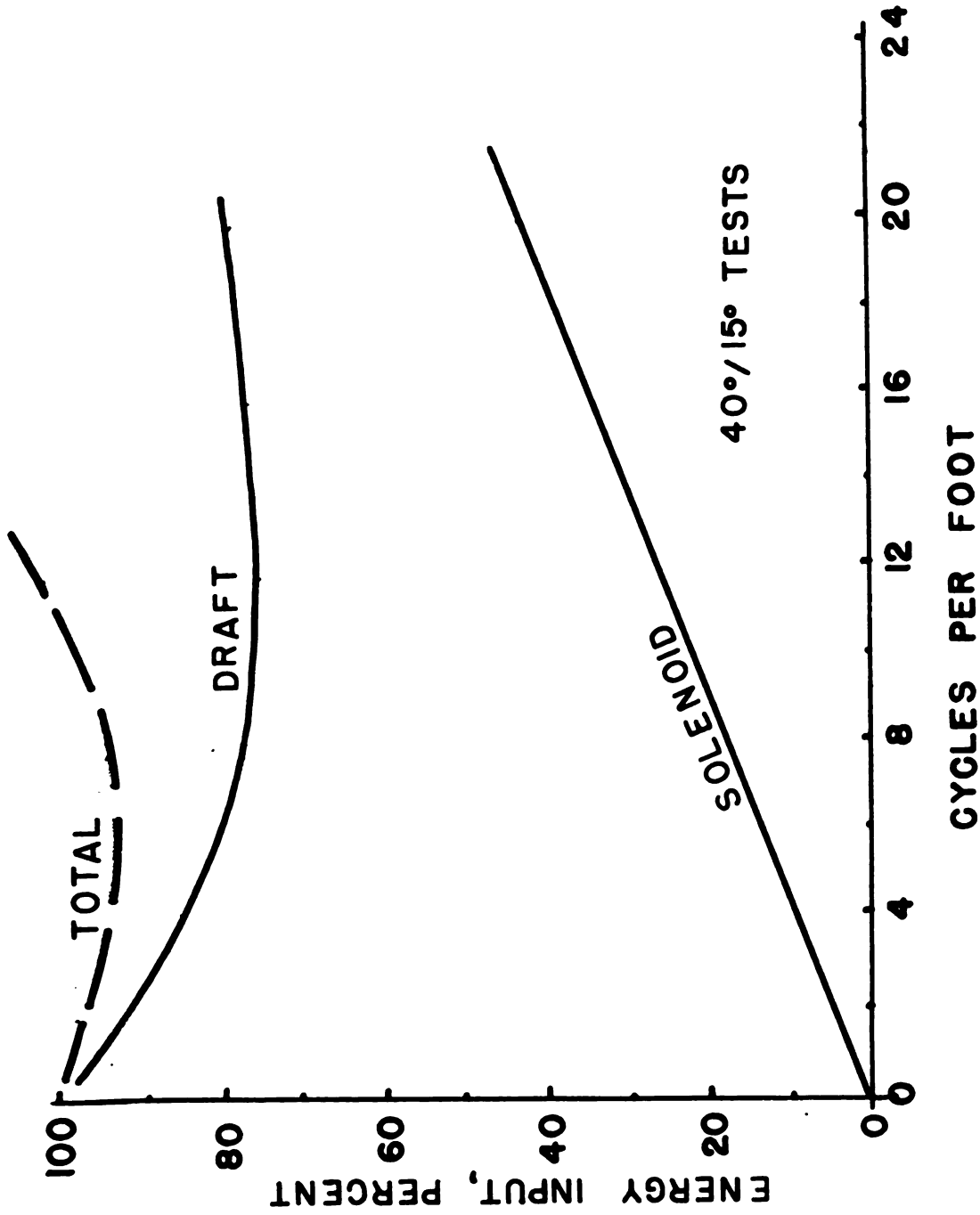


Figure 41. Percent energy applied by draft and solenoid action of a vibrating tool compared to a rigid tool where $\delta = 40^\circ$ and $\gamma = 15^\circ$ at 17.5% soil moisture.

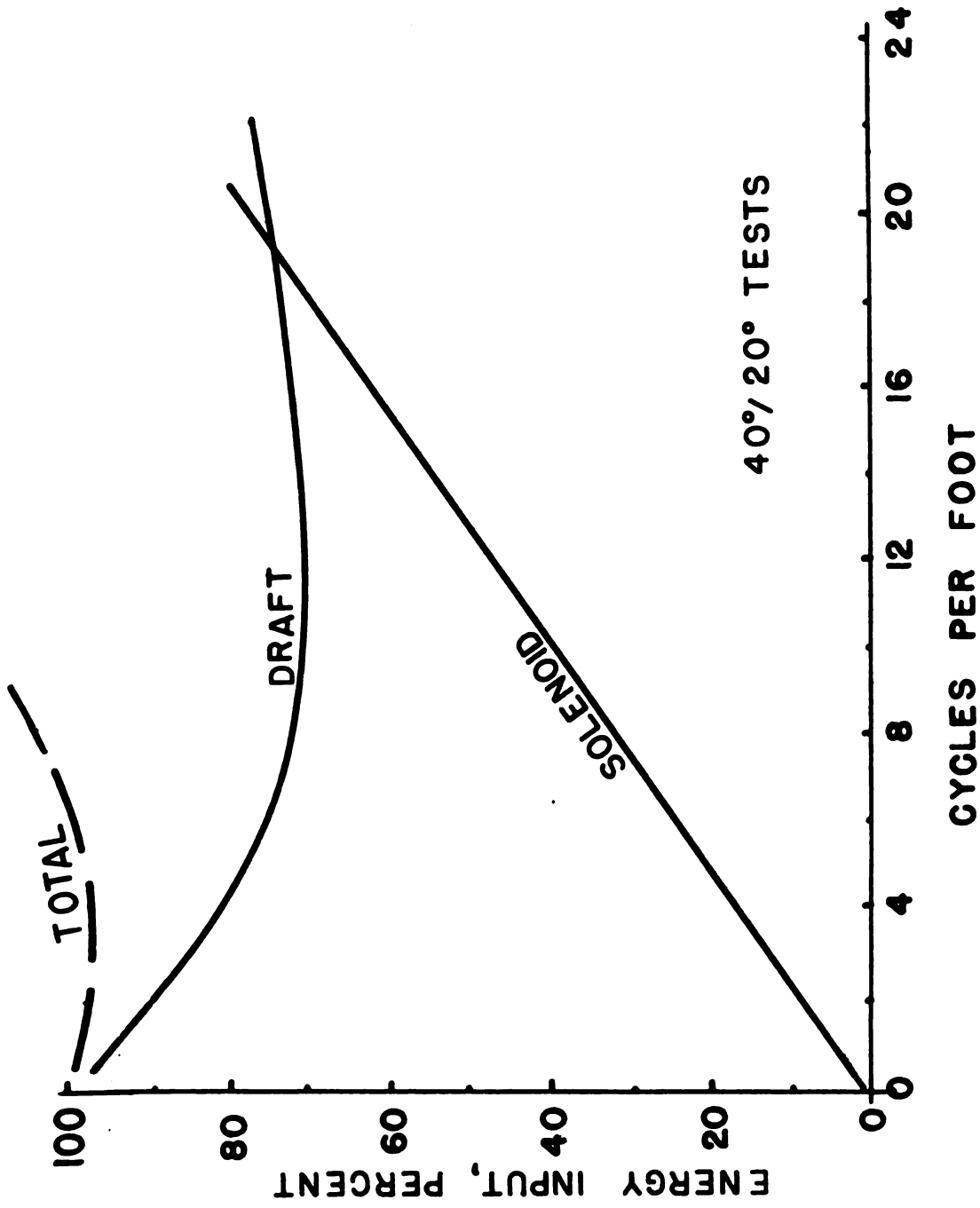


Figure 42. Percent energy applied by draft and solenoid action of a vibrating tool compared to a rigid tool where $\delta = 40^\circ$ and $\lambda = 20^\circ$ at 17.5 % soil moisture.

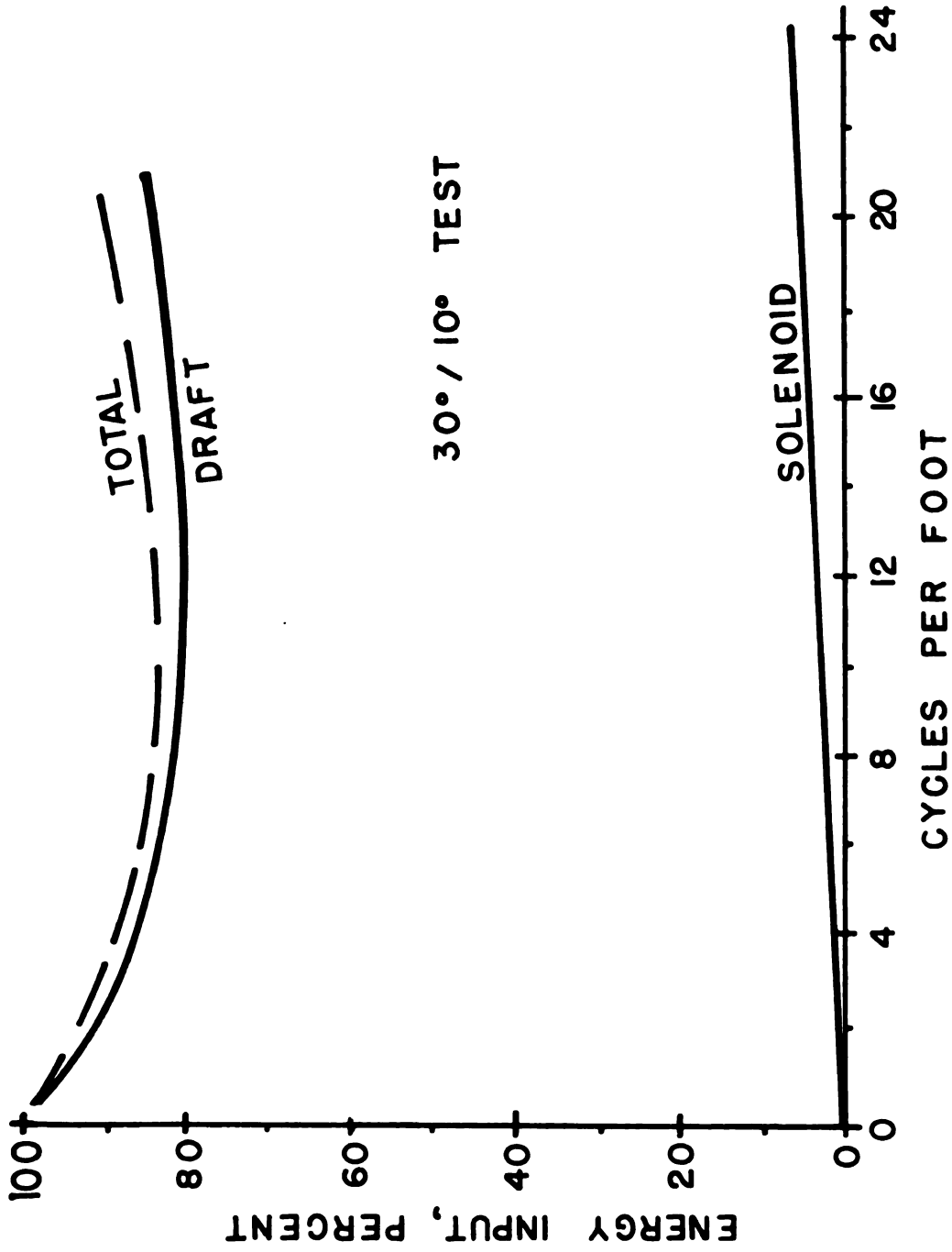


Figure 43. Percent energy applied by draft and solenoid action of a vibrating tool compared to a rigid tool where $\delta = 30^\circ$ and $\beta = 10^\circ$ at 17.5% soil moisture.

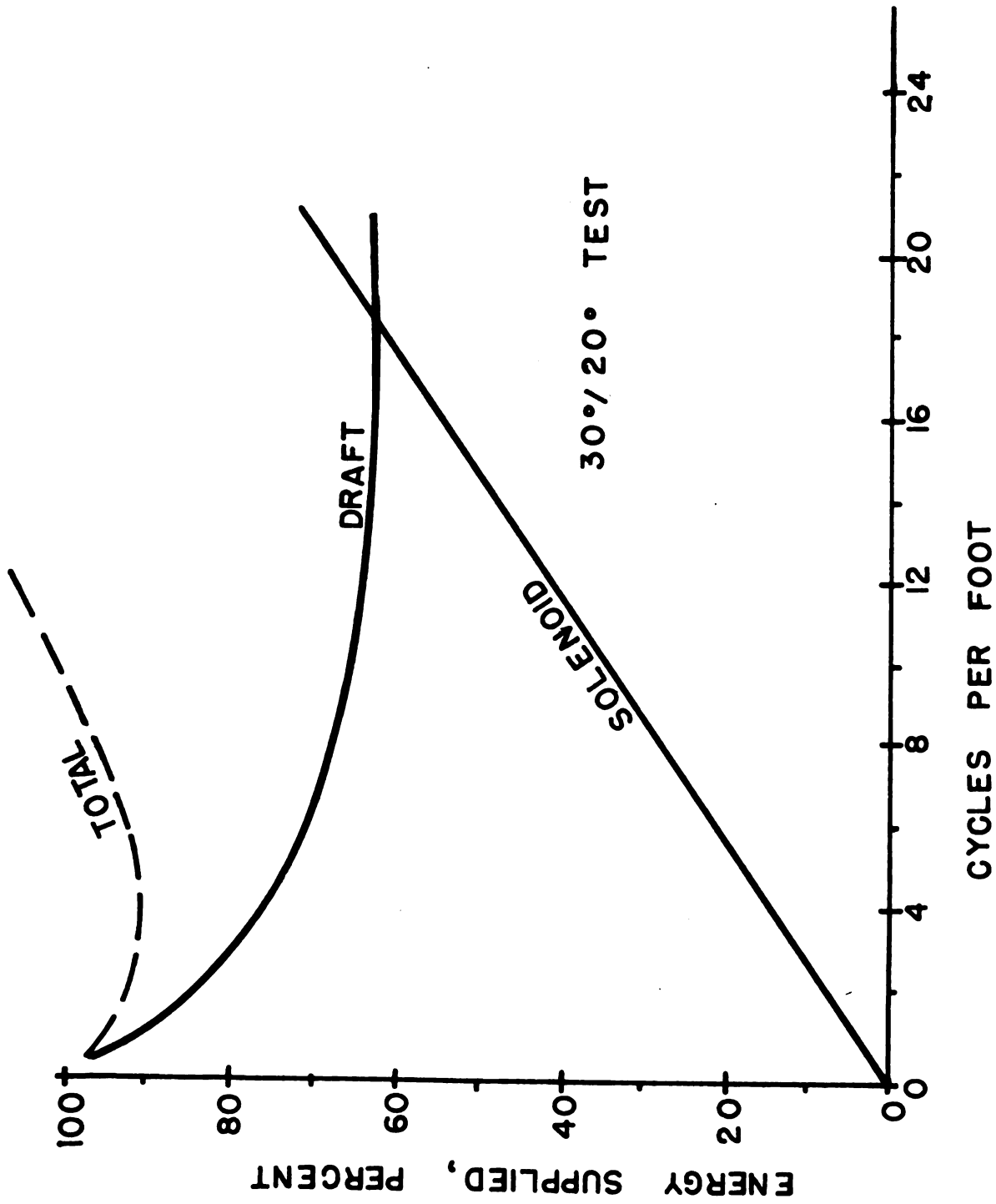


Figure 44. Percent energy applied by draft and solenoid action of a vibrating tool compared to a rigid tool where $\delta = 30^\circ$ and $\gamma = 20^\circ$ at 17.5% soil moisture.

SUMMARY

Laboratory tests were conducted in a mobile soil bin to determine the draft and energy requirements of a simple vibrating tillage tool. The draft and the energy requirements of a rigid and of a vibrating tool were compared.

Equipment was built and instrumentation was developed to determine the various components of the soil forces acting upon a tillage tool, and to locate the point of application of the resultant soil force on a flat tool.

A strain gage dynamometer was used to measure the resultant soil forces on the tool, and pressure cells were mounted in the surface of the tool to measure the normal force exerted by the soil.

Tests were conducted to determine the amount of force required to merely cut the soil in an effort to determine that portion of the draft force required to separate the soil slice.

The vibrating tool was a simple inclined plane, mounted in such a way that the leading edge could be forced upward about a horizontal axis through its trailing edge. The tool was powered by an electric solenoid. The rigid tool was simply the above tool locked in position.

The draft of the vibrating tillage tool (compared with the rigid tool) decreased rapidly as the vibrational frequency approached the natural shear plane frequency of a rigid tool; beyond that frequency the draft reduction was

slight. The energy requirement of a vibrating tillage tool was computed on the basis of the draft force and the energy provided by the vibrating mechanism. The energy requirement of the vibrating tool was in general less than that of a rigid tool at low frequencies, and exceeded the rigid tool energy as the frequency was increased.

The draft reduction was generally greater for larger amplitudes of vibration and for soil with a higher shear strength.

Better soil crumbling was observed with the vibrating tool than with the rigid tool, which may lead to seedbed preparation in a single field operation.

CONCLUSIONS AND OBSERVATIONS

Conclusions.

1. The draft of a simple tillage tool can be reduced by pivot mounting the tool in order that the leading edge can be swung upward to cause soil failure.
2. The draft decreased as the frequency of vibration was increased up to the natural frequency of shear plane formation for a rigid tool. Beyond that frequency, the draft reduction was slight. Other factors affecting the amount of draft reduction were soil physical properties and magnitude of tool movement.
3. Vibrating the tool did not materially reduce the total tillage energy requirement of the soil.
4. Approximately 50 % of the total draft force of a rigid tool of the type used in these tests can be attributed to the cutting force on the leading edge of the tool.
5. The instrumentation and methods developed in this study can be used for further studies of vibrating tillage tools.

Observations.

1. Since the resistance to cutting soil increases only slightly with an increase in speed, a mode of vibration which prevents the tool from cutting during a portion of the tillage cycle should further reduce draft.

2. Better soil crumbling was observed when the vibrating tool was used. Therefore, a vibrating blade can be used to control clod size and thus reduce the need for secondary tillage operations.
3. An analysis of the efficiency of a vibrating tillage tool based on the mean clod size will probably show that the vibrating tool is a more efficient tillage tool than this study or previous investigations have actually indicated.

SUGGESTIONS FOR FURTHER INVESTIGATIONS

1. Studies should be conducted to determine the effect of vibrations on the values of cohesion and internal angle of friction of soils.
2. A study should be made in which the efficiency of operation of a vibrating tillage tool is based on soil clod size reduction.
3. Methods should be devised to measure the forces acting in a soil mass during the operation of rigid and vibrating tillage tools.
4. A technique should be developed to measure more completely the normal and tangential forces acting on the surface of a tillage tool.
5. Vibrating tillage tools employing many different modes of vibration should be studied.
6. Tests using the present tillage tool should be conducted in various soil types to further study the effect of the soil parameters upon draft reduction and energy requirements.
7. Study the possibility of applying mechanical movement to a plow body from a separate power source.

REFERENCES

- Austin, E. W. (1948). Earth-mover blade with vibrating attachment. U. S. Patent Office No. 2,443,492.
- Brewer, C. A. (1927). Soil-vibrating apparatus. U. S. Patent Office No. 1,614,273.
- Casagrande, A. and Shannon, W. L. (1948). Stress-deformation and strength characteristics of soils under dynamic loads. Proc. of the Second Internatl. Conf. on Soil Mech. and Found. Engr., Vol. 5, p. 29.
- _____. (1948). Research on stress-deformation and strength characteristics of soils and soft-rocks under transient loading. Harvard Grad. School of Engr. Bul. 448.
- Demenlaere, G. (1936). Plow. U. S. Patent Office No. 2,087,639.
- Dubrovskii, A. A. (1956). Influence of vibrating the tools of cultivating implements upon draft resistance. Shornik Trud. semled Mekhan. Lenin Akad. selko z. Nauk (Caterpillar Translation No. 221).
- Eggenmuller, A. (1958). Versuche mit Gruppen gegeneinander schwingender Hackwerkzeuge (Experiments with alternately oscillating hoe tines). Grndl. Landtech., Heft 10, p. 70 (Caterpillar Translation No. 221).
- _____. (1958). Feldversuche mit einem schwingenden Pflugkorper (Field experiments with an oscillating plow body). Grndl. Landtech., Heft 10, p. 79 (Caterpillar Translation No. 221).
- _____. (1958). Untersuchungen an schwingenden Hanfelkorpern (Investigations on oscillating ridging bodies). Grndl. Landtech., Heft 10, p. 143 (Caterpillar Translation No. 221).
- _____. (1958). Schwingende bodenbearbeitungswerkzeuge: kinematik und versuche mit einzelnen modellwerkzeugen (Oscillating implements: Kinematics and experiments with models of individual tools). Grndl. Landtech., Heft 10, p. 55 (Caterpillar Translation No. 221).
- Garst, D. (1914). Means for clearing the surface of dirt working tools. U. S. Patent Office No. 2,087,639.

- Gill, W. R. and McCreery, W. F. (1959). The effect of the size of cut of two types of tillage tools on clod size and efficiency of operation. Paper presented at 1959 Winter A.S.A.E. Meeting, Chicago, Ill., Dec. 15 - 18.
- Gunn, Jack T. and Tramontini, V. N. (1955). Oscillation of tillage implements. Agr. Engr., Vol. 36, No. 11, p. 725.
- Harris, W. L. (1960). Dynamic Stress Transducers and the Use of Continuum Mechanics in the Study of Various Stress Strain Relationships. Unpub. Ph. D. Thesis, Michigan State University, East Lansing.
- Hendrick, James G. (1961). Strength and energy relations of a dynamically loaded clay soil. Transactions of the A.S.A.E., Vol. 4, No. 1, p. 31.
- Hendrick, James G. (1962). The tillage energy of a vibrating tillage tool. Paper presented at the Annual Summer Meeting of A.S.A.E., Washington, D. C., June 17 - 20.
- Hubert, L. A. (1909). Gang plow. U. S. Patent Office No. 939,132.
- Kaburaki, H. and Kisu, M. (1959). Studies on cutting characteristics of ploughs. Jour. of the Kanto-Tosan Agr. Exp. Sta., No. 12 (NIAE Translation No. 79).
- Koudner, R. L. (1960). A Non-Dimensional Approach to the Vibratory Cutting, Compaction, and Penetration of Soils. The Johns Hopkins Univ., Baltimore, Md. 183 pp.
- Lambe, T. W. (1951). Soil Testing for Engineers. Chapt. XIII, John Wiley and Sons, N. Y., p. 93.
- National Tillage Machinery Laboratory (1961). Soil-tool Relationships. A portion of the N.T.M.L. 1961 Annual Report.
- Nichols, M. L. (1931). The dynamic properties of soils, II. Soil and metal friction. Agric. Engr., Vol. 12, No. 8, p. 321.
- Payne, P. C. J. (1956). The relationship between the mechanical properties of soil and the performance of simple cultivation implements. Jour. of Agr. Engr. Research, Vol. 1, No. 1, p. 23.

Rhoten, C. M. (1950). Heating and vibrating means for plow moldboards. U. S. Patent Office No. 2,641,173.

Seed, H. B. and Lundgren, R. (1954). Investigation of the effect of transient loading on the strength and deformation characteristics of saturated sands. ASTM Proc., Vol. 54, p. 1288.

Shkurenko, N. S. (1960). Experimental data on the effect of oscillation on the cutting resistance of soil. J. of Agric. Engr. Res., Vol. 5, No. 2, p. 226.

Soehne, W. (1956). Einige Grundlagen fur eine Landtechnische Bodenmechanik (Some basic considerations of soil mechanics as applied to agricultural engineering). Grndl. der Landtech., Heft 7, p. 11 (NIAE Translation No. 53).

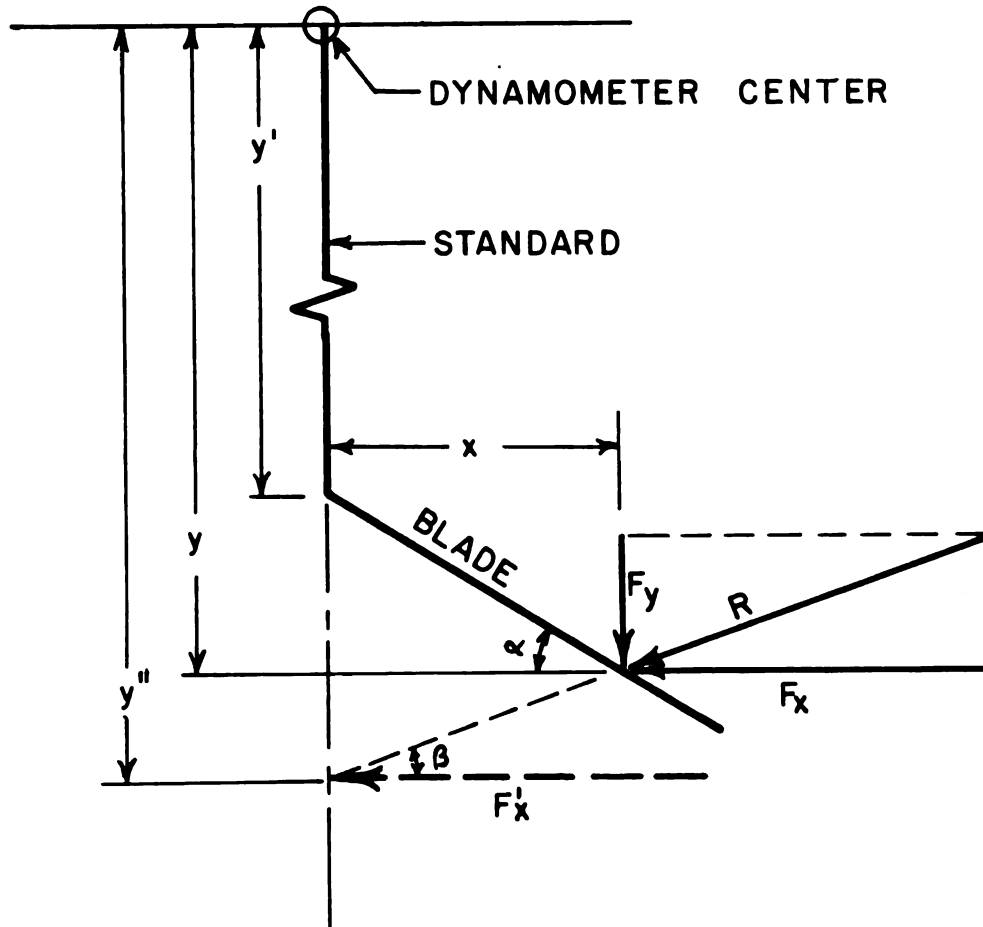
Stong, Jack V. (1960). Basic Factors Affecting the Strength and Sinkage of Tillable Soils. Unpub. M. S. Thesis, Michigan State University, East Lansing.

Taylor, D. W. and Whitman, R. V. (1954). The Behavior of Soils Under Dynamic Loadings. Rpt. No. 3, Mass. Inst. of Tech., Soil Mech. Lab., Boston.

Terzaghi, Karl (1953). Theoretical Soil Mechanics. John Wiley and Sons, New York.

APPENDIX A

SAMPLE PROBLEM



Given: $F_x = 10 \text{ lb.}$, $F_y = 4 \text{ lb.}$, $M = 120 \text{ in-lb.}$, $\alpha = 30^\circ$,
 $y' = 10''$

Find: Resultant force (R) and point of application on the blade (x and y).

Solution: 1) $R = \sqrt{F_x^2 + F_y^2} = 10.8 \text{ lb.}$

2) Equation of the plane of the blade:

$$y = y' + x \tan \alpha \quad \dots \dots \dots (a)$$

3) Equation of the resultant force direction:

$$y = y'' - x \tan \beta \quad \dots \dots \dots (b)$$

4) Solving (a) and (b) for x and y:

$$y' + x \tan \alpha = y'' - x \tan \beta$$

$$y = y' + x \tan \alpha$$

$$x = \frac{y'' - y'}{\tan \alpha + \tan \beta}$$

$$\tan\beta = \frac{F_y}{F_x} = 0.40$$

$$\tan\alpha = 0.58$$

$$y'' = \frac{M}{F_x} = \frac{120}{10} = 12.0''$$

$$x = \frac{12.0 - 10.0}{.58 + .40} = 2.06''$$

$$y = 10.0 + (2.06)(0.58) = 11.2''$$

APPENDIX B

TABLE 1

Dynamometer and Pressure Cell Calibration Information
(Brush Model 520 Amplifiers)

Recorded Force	Calibration		Operation	
	Attenuator Setting	mm Deflection	Attenuator Setting	mm per Unit Load
<u>Dynamometer:</u>				
Draft (F_x)	2	32.5	2	2 lb/mm
Vertical (F_y)	2	33.5	2	2 lb/mm
Moment (M)	5	19.0	5	2 ft-lb/mm
<u>Pressure Cells:</u>				
# 1	5	21.3	2	0.5 psi/mm
# 2	5	21.9	2	0.5 psi/mm
# 3	5	17.0	2	0.5 psi/mm
# 4	5	15.2	2	0.5 psi/mm
# 5	5	29.8	2	0.5 psi/mm

TABLE 2

Tool Pressure Cell Calibration

Applied Pressure		Chart Reading (mm Deflection)				
psi	in. Hg	Cell # 1	Cell # 2	Cell # 3	Cell # 4	Cell # 5
1	2-1/32	1.8	2.0	2.0	2.0	2.0
		1.8	2.0	2.0	1.8	2.0
		2.0	2.0	1.8	1.9	2.0
		2.0	2.0	1.9	1.8	1.8
2	4-1/16	3.8	4.0	4.0	3.8	3.8
		4.0	4.0	4.0	3.8	3.9
		4.0	4.0	3.8	3.7	3.8
		3.6	4.0	3.8	3.8	4.0
3	6-1/8	5.8	5.7	6.0	5.5	5.5
		5.5	5.8	6.0	5.5	5.5
		5.6	5.9	5.8	5.5	5.5
		5.7	6.0	5.9	5.5	5.9
4	8-5/32	7.5	7.6	7.8	7.5	7.3
		7.5	7.9	8.0	7.5	7.5
		7.8	8.0	7.5	7.0	7.8
		7.6	8.0	7.6	7.5	7.5
5	10-3/16	9.5	9.8	9.8	9.6	9.6
		9.5	9.8	10.0	9.5	9.6
		9.5	9.9	9.5	9.3	10.0
		9.7	9.9	9.7	9.3	9.0
7.5	5-1/4	14.5	14.7	15.0	14.7	14.3
		14.5	14.9	15.0	14.5	14.0
		14.5	14.9	15.0	14.5	15.0
		14.5	14.9	14.7	14.5	14.0
10	20-3/8	20.0	20.0	20.2	20.0	20.0
		20.0	20.0	20.5	19.8	19.5
		20.0	19.7	20.0	20.0	21.0
		19.8	19.9	20.0	20.0	19.5
12.5	25-13/32	25.5	25.0	25.5	25.0	25.0
		25.5	24.5	25.7	25.5	25.0
		25.5	24.9	25.5	25.8	26.5
		25.0	24.6	25.0	25.5	25.0
15	30-1/2	31.0	30.0	31.0	30.5	30.5
		31.5	30.0	31.5	31.6	30.5
		31.0	30.0	30.5	31.5	32.0
		30.0	30.0	30.0	31.5	30.5

TABLE 3

Normal Load vs. Tangential Force for Mild Steel
and Teflon at Various Moisture Contents

Moisture (%)	Normal* Load (lb.)	Tangential Force (lb.)	
		Steel	Teflon
0.65	2.20	1.05	0.65
		1.00	0.60
		0.85	0.55
		2.60	1.45
	5.20	2.60	1.45
		2.65	1.50
		3.70	1.90
		3.60	1.90
	7.20	3.50	1.90
		0.95	0.60
6.0	2.20	0.85	0.65
		0.90	0.60
		2.10	1.40
		2.10	1.30
	5.20	2.10	1.40
		3.10	2.00
		2.90	1.90
		2.80	2.81
	7.20	0.65	0.55
		0.70	0.65
9.1	2.20	0.70	0.70
		1.50	1.45
		1.50	1.40
		1.55	1.45
	5.20	3.00	2.10
		2.60	1.80
		2.80	2.00
		0.70	0.60
	7.20	0.65	0.45
		0.85	0.57
11.4	2.20	1.90	1.20
		1.80	1.20
		1.90	1.10
		2.30	1.45
	5.20	2.45	1.50
		2.30	1.40
		1.30	0.80
		1.20	0.70
	7.20	1.10	0.70
		2.50	1.40
15.1	2.20	2.50	1.55
		2.50	1.60
		3.40	2.20
		3.50	2.10
	5.20	3.50	2.15

TABLE 3 (continued)

Moisture (%)	Normal* Load (lb.)	Tangential Force (lb.)	
		Steel	Teflon
19.7	2.20	1.05	0.80
		1.10	1.00
		1.10	0.80
	5.20	2.20	1.60
		2.10	1.60
		2.15	1.65
		2.70	1.85
	7.20	3.00	2.20
		2.60	2.20
		0.60	0.70
26.5	2.20	0.50	0.55
		0.70	0.70
		1.00	1.10
	5.2	1.20	1.20
		1.00	1.30

* Cross-sectional area of the soil sample = 0.74 in^2 .

** At 26.5 % moisture, water was squeezed from the sample at 5.2 # Normal Load.

TABLE 4

Force Exerted on the Blade by the Solenoid

Material Actuated	Working Angle (°)	Displacement Angle (°)	Solenoid Movement (in.)	Maximum Force (lb.)
Blade Alone	30	10	.19	19
	30	15	.25	25
	30	20	.38	39
	40	10	.19	18
	40	15	.25	22
	40	20	.38	31
Blade in Loose Soil	30	10	.19	22
	30	15	.25	38
	30	20	.38	55
	40	10	.19	23
	40	15	.25	33
	40	20	.38	48
Blade in Compact Soil (1.12 gm/cc)	30	10	.19	24
	30	15	.25	47
	30	20	.38	61
	40	10	.19	25
	40	15	.25	46
	40	20	.38	63
(1.23 gm/cc)	30	10	.19	26
	30	15	.25	56
	30	20	.38	73
	40	10	.19	26
	40	15	.25	55
	40	20	.38	70

TABLE 5

Average Draft Values for a Rigid
Tool Run at 30° and 40° Working Angles

Working Angle (°)	Bulk Density (gm/cc)	Percent Moisture	Forward Speed (fps)	Average Draft (lb.)	Standard Deviation (lb.)
30	1.12	14	1	6.2	1.3
30	1.12	14	2	8.1	2.0
30	1.23	14	1	9.8	1.5
30	1.23	14	2	11.6	2.7
40	1.12	14	1	8.8	1.6
40	1.12	14	2	10.1	1.3
40	1.23	14	1	10.0	1.1
40	1.23	14	2	11.8	1.9
30	1.12	17.5	1	13.2	2.6
30	1.12	17.5	2	9.5	1.6
30	1.12	17.5	4	12.9	2.0
30	1.23	17.5	1	15.9	2.4
30	1.23	17.5	2	18.4	2.5
40	1.12	17.5	1	12.2	3.5
40	1.12	17.5	2	16.5	4.4
40	1.23	17.5	1	15.1	2.6
40	1.23	17.5	2	18.0	2.4

TABLE 6

Energy Transmitted to the Blade by
the Solenoid in Soil at 17.5 % Moisture

Working Angle (°)	Displacement Angle (°)	Energy per Cycle (ft-lb)			
		Bare Tool	Loose Soil	Compact Soil	
				1.12 gm/cc	1.23 gm/cc
30	10	0.19	0.21	0.23	0.25
	15	0.42	0.51	0.62	0.74
	20	0.87	1.12	1.24	1.48
40	10	0.16	0.23	0.25	0.28
	15	0.44	0.54	0.65	0.78
	20	0.92	1.20	1.35	1.62

TABLE 7

Relative Draft Data for a Working Angle (δ) of 40° and 14 % Soil Moisture

Displacement Angle ($^\circ$)	Bin Speed (fps)	Soil Density (gm/cc)	Vibrational Frequency (cps)	Vibrating Draft Force Rigid Draft Force (dimensionless)
10	1	1.12	4	.82
10	1	1.12	8	.82
10	1	1.12	21	.54
10	1	1.12	4	.90
10	1	1.12	8	.89
10	1	1.12	11	.86
10	1	1.12	21	.74
10	2	1.12	4	1.11
10	2	1.12	8	.86
10	2	1.12	21	.70
10	2	1.23	4	.94
10	2	1.23	6	.92
10	2	1.23	8	.95
10	2	1.23	10	.92
10	2	1.23	12	.94
10	2	1.23	21	.78
10	4	1.12	4	.89
10	4	1.12	8	.90
10	4	1.12	21	.85
15	1	1.12	4	.77
15	1	1.12	6	.75
15	1	1.12	8	.82
15	1	1.12	21	.74
15	1	1.23	4	.91
15	1	1.23	7	.85
15	1	1.23	15	.62
15	1	1.23	21	.90

TABLE 7 (continued)

Displacement Angle (°)	Bin Speed (fps)	Soil Density (gm/cc)	Vibrational Frequency (cps)	<u>Vibrating Draft Force</u> <u>Rigid Draft Force</u> (dimensionless)
15	2	1.23	4	.74
15	2	1.23	8	.87
15	2	1.23	21	.97
20	1	1.23	4	.95
20	1	1.23	8	.80
20	1	1.23	21	.65
20	2	1.23	4	.99
20	2	1.23	8	.84
20	2	1.23	21	.82

TABLE 8
Relative Draft Data for a Working Angle (δ) of 40° and 17.5 % Soil Moisture

Displacement Angle (γ)	Bin Speed (fps)	Bulk Density (gm/cc)	Vibrational Frequency (cps)	<u>Vibratory Draft Force</u> <u>Rigid Draft Force</u> (dimensionless)
10	1	1.12	4	.87
10	1	1.12	8	.95
10	1	1.12	12	1.12
10	1	1.12	21	1.04
10	2	1.12	4	.93
10	2	1.12	8	.87
10	2	1.12	12	.82
10	2	1.12	21	.91
10	4	1.12	8	.91
10	4	1.12	21	.97
10	1	1.23	4	.97
10	1	1.23	8	.77
10	1	1.23	12	.77
10	1	1.23	21	.82
10	2	1.23	4	.76
10	2	1.23	8	.89
10	2	1.23	21	.76
15	1	1.12	4	.92
15	1	1.12	8	.94
15	1	1.12	12	.84
15	1	1.12	21	.88
15	2	1.12	4	.96
15	2	1.12	8	.94
15	2	1.12	21	1.00
15	1	1.23	4	.87
15	1	1.23	8	.80

TABLE 8 (continued)

Displacement Angle (°)	Bin Speed (fps)	Bulk Density (gm/cc)	Vibrational Frequency (cps)	<u>Vibratory Draft Force</u> <u>Rigid Draft Force</u> (dimensionless)
15	1	1.23	12	.85
15	1	1.23	21	.85
15	2	1.23	4	.89
15	2	1.23	8	.86
15	2	1.23	12	.97
20	1	1.12	4	.72
20	1	1.12	8	.64
20	1	1.12	12	.73
20	1	1.12	21	.69
20	1	1.23	4	.85
20	1	1.23	8	.74
20	1	1.23	12	.82
20	2	1.12	4	.81
20	2	1.12	8	.73
20	2	1.23	4	.87
20	2	1.23	8	.93
20	2	1.23	12	.85
20	2	1.23	21	.92

TABLE 9

Relative Draft Data for a Working Angle (δ) of 30° and 14.0 % Soil Moisture

Displacement Angle (γ)	Bin Speed (fps)	Soil Density (gm/cc)	Vibrational Frequency (cps)	Vibrating Draft Force Rigid Draft Force (dimensionless)
5	1	1.23	4	.97
5	1	1.23	8	.95
5	1	1.23	12	.88
5	1	1.23	21	.87
5	2	1.23	4	.95
5	2	1.23	8	.88
5	2	1.23	13	.97
5	2	1.23	21	.97
5	1	1.12	4	.89
10	1	1.12	8	.96
10	1	1.12	21	.85
10	1	1.23	4	.95
10	1	1.23	6	.88
10	1	1.23	8	.70
10	1	1.23	15	.76
10	1	1.23	21	.78
10	2	1.12	8	.95
10	2	1.12	21	.81
10	2	1.23	4	1.11
10	2	1.23	8	.82
10	2	1.23	10	.81
10	2	1.23	12	.75
10	2	1.23	21	.61
15	1	1.12	4	.78
15	1	1.12	8	.87
15	1	1.12	5	.91

TABLE 9 (continued)

Displacement Angle ($^{\circ}$)	Bin Speed (fps)	Soil Density (gm/cc)	Vibrational Frequency (cps)	<u>Vibrating Draft Force</u> <u>Rigid Draft Force</u> (dimensionless)
15	2	1.12	4	.88
15	2	1.12	8	.77
15	2	1.12	21	.74
15	2	1.23	4	.90
15	2	1.23	8	.80
15	2	1.23	21	.71
20	1	1.23	4	.99
20	1	1.23	6	.81
20	1	1.23	8	.84
20	1	1.23	12	.76
20	1	1.23	21	.88
20	1	1.12	4	.81
20	1	1.12	8	.81
20	1	1.12	21	.78
20	2	1.12	4	.97
20	2	1.12	8	.89
20	2	1.12	12	.77
20	2	1.12	21	.72
20	4	1.23	4	.84
20	4	1.23	8	.92
20	4	1.23	21	.82

TABLE 10
Relative Draft Data for a Working Angle (δ) of 30° and 17.5 % Soil Moisture

Displacement Angle ($^\circ$)	Bin Speed (fps)	Bulk Density (gm/cc)	Vibrational Frequency (cps)	<u>Vibratory Draft Force</u> <u>Rigid Draft Force</u> (dimensionless)
5	1	1.12	4	.95
5	1	1.12	8	.93
5	1	1.12	10	.96
5	1	1.12	13	.98
10	1	1.12	4	.86
10	1	1.12	6	.76
10	1	1.12	8	.81
10	1	1.12	21	.79
10	2	1.23	4	.75
10	2	1.23	8	.79
10	2	1.23	21	.72
20	1	1.12	4	.75
20	1	1.12	8	.72
20	1	1.12	21	.59
20	2	1.12	4	.79
20	2	1.12	8	.75
20	2	1.12	21	.66
20	4	1.12	4	.88
20	4	1.12	8	.86
20	4	1.12	11	.77
20	4	1.12	21	.73
20	1	1.23	4	.67
20	1	1.23	8	.75
20	1	1.23	21	.65
20	2	1.23	4	.78
20	2	1.23	8	.88
20	2	1.23	21	.63

TABLE 11

Tabulation of Values Used for Comparing Measured Draft Force
and Computed Draft Force for a Rigid Blade ($\delta = 40^\circ$)

Test	Cell Pressure					q	F _x (cal.)	F _x (rec.)	$\frac{F_x \text{ (cal.)}}{F_x \text{ (rec.)}}$
	1	2	3	4	5				
23/4/13 a M	5.5	2.5	2.5	2.3	2.0	.89	45.5	45	1.01
23/4/13 a A	3.0	1.3	1.0	1.7	0.6	.91	31.0	31	1.00
23/4/13 b M	5.5	2.5	3.0	1.2	2.0	.71	40.4	47	.86
23/4/13 b A	4.0	1.6	2.0	0.7	1.2	.68	32.1	37	.87
23/4/12 a M	3.5	2.0	1.5	1.5	1.5	.80	33.3	38	.88
23/4/12 a A	2.0	1.5	1.2	1.2	0.7	.71	25.8	28	.92
23/4/12 b M	6.5	2.5	1.7	1.0	2.0	.68	40.1	48	.84
23/4/12 b A	2.5	1.5	1.0	1.3	0.5	.68	25.3	35	.72
23/4/11 a M	7.0	2.5	3.0	1.0	2.0	.68	42.9	40	1.07
23/4/11 a A	2.0	1.6	2.2	0.8	0.9	.63	27.9	30	.93

Mechanical Analysis:

Fine Gravel	1.2	%
Coarse Sand	3.6	%
Medium Sand		
Fine Sand	26.8	%
Very Fine Sand	27.7	%
50 Micron	13.4	%
5 Micron	5.6	%
2 Micron	15.6	%
Hygroscopic Coefficient	1.6	%
Moisture Equivalent	14.3	%
Maximum Water Holding Capacity	63.8	%
Soil Saturated	37.1	%
60 cm Tension	25.4	%
Permanent Wilting Point	8.7	%
Lower Plastic Limit	21.0	%
Upper Plastic Limit	25.5	%
Plastic Range	4.5	%
Density	2.6	%

TABLE 13

Bevamer Penatrometer Sinkage Data

Bulk Density (gm/cc)	Soil Moisture (%)	Penatrometer Diameter (in.)	Sinkage (in.)	Force (lb.)
1.12	17.5	1	1	20
			2	30
			3	40
			4	62
		2	1	50
			2	80
			3	132
			4	210
1.23	17.5	1	1	27
			2	37
			3	54
			4	80
		2	1	75
			2	110
			3	180
			4	280
1.12	14.0	1.5	0.5	28
			1	41
			2	61
			3	93
		2.5	0.5	53
			1	84
			2	143
			3	178
1.23	14.0	1	0.5	35
			1	38
			2	40
			3	70
		2	0.5	55
			1	75
			2	115
			3	167

MICHIGAN STATE UNIVERSITY LIBRARIES



3 1293 03085 1426